MG132 (Calbiochem- Novabiochem, San Diego, CA) for 8 hours before preparation of the crude membrane. Crude membrane fractions were prepared 48 hours after infection. The specimens were separated via 7% SDS-PAGE and were subjected to Western blot analysis with a 1,000-fold diluted polyclonal human BSEP antibody as previously described.[15]

To examine BSEP expression on the cell surface, cell surface biotinylation was performed as follows. MDCK II cells were seeded 24 hours before infection in a 12-well plate at a density of 4×10^5 cells per well and were infected with the recombinant adenoviruses at 250 MOI. Cells were washed twice with ice-cold phosphate-buffered saline (PBS) containing 0.1 mmol/L $CaCl_2$ and 1 mmol/L $MgCl_2$ (PBS-Ca/Mg) 48 hours after infection and incubated twice with NHS-SS-biotin (Pierce Biotechnology, Rockford, IL) at 4°C for 30 minutes. After removing the NHS-SS-biotin, the cells were washed with PBS-Ca/Mg containing 100 mmol/L glycine and incubated at 4°C for 15 minutes, then disrupted with 100 μL lysis buffer (50 mmol/L Tris, 150 mmol/L NaCl, 5 mmol/L ethylenediaminetetraacetic acid, 1% Triton-X100 [pH 7.5]) containing 1% SDS and 0.1 mmol/L phenylmethylsulfonyl fluoride at 4°C for 15 minutes. Then, 50 μL aliquots were preserved as whole cell lysate, and the remaining aliquots (50 μL) were diluted with 450 μL lysis buffer containing 1% SDS and 0.1 mmol/L phenylmethylsulfonyl fluoride to reduce the SDS concentration. Streptavidin-agarose beads (Pierce Biotechnology) were then added to the lysate, followed by incubation at 4°C overnight with end-over-end rotation. The beads were washed three times with lysis buffer, twice with high-salt lysis buffer (50 mmol/L Tris, 500 mmol/L NaCl, 5 mmol/L ethylenediaminetetraacetic acid, 0.1 % Triton-X 100 [pH 7.5]), and once with low-salt lysis buffer (50 mmol/L Tris [pH 7.5]). The biotinylated proteins were eluted with 30 μL 3 × SDS loading buffer (Biolabs, Hertfordshire, UK) diluted to 1 × SDS with PBS at 60°C for 5 minutes. The biotinylated proteins (30 μL) and total cell lysate (30 μL) were subjected to Western blot analysis.

To examine the extent of glycosylation of BSEP, peptide N-glycosidase F (New England Biolabs, Beverly, MA) digestions were performed at 37°C for 2 hours as described by the manufacturer. The deglycosylated proteins were subjected to Western blot analysis.

Immunofluorescence. To determine the localization of BSEP, MDCK II cells were seeded on glass coverslips 24 hours before infection at a density of 3×10^5 cells/well in 12-well plates and were infected with recombinant adenoviruses at 25 MOI (wild-type and E297G BSEP) or 250 MOI (D482G BSEP). Cells were fixed with 100% methanol at −20°C for 10 minutes 48 hours after the infection, and were permeabilized in 1% Triton X-100 (Sigma, St. Louis, MO) in PBS for 5 minutes. After permeabilization, cells were incubated with 100-fold diluted polyclonal human BSEP antibodies at 4°C for 16 hours and then with 250-fold diluted Alexa Flour 488 donkey anti-goat immunoglobulin G at room temperature for 1 hour. Confocal laser scanning was performed using an LSM 510 apparatus (Carl Zeiss, Oberkochen, Germany).

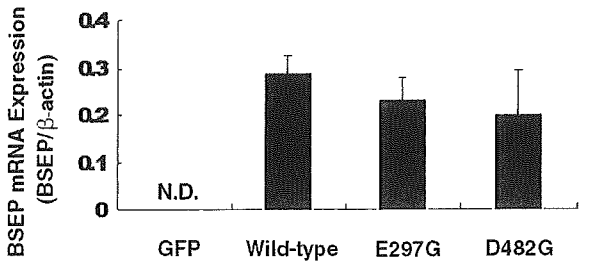

Fig. 1. Determination of expression levels of BSEP mRNA. RNA was isolated from MDCK II cells 48 hours after infection by recombinant adenoviruses at 50 MOI. Real-time quantitative PCR was performed as described in Materials and Methods. BSEP gene expression in each reaction was normalized by the expression of β-actin. Horizontal bars represent the mean ± SE of triplicate determinations. BSEP, bile salt export pump; mRNA, messener RNA; N.D., not detected; GFP, green fluorescence protein.

Transport Assays. To determine the transport function of BSEP, HEK 293 cells were seeded 72 hours before infection at a density of 4.0×10^6 cells per 15-cm dish and were infected with recombinant human BSEP adenovirus at 25 MOI. Crude membrane fractions[16] and isolated membrane vesicles[14] were prepared 48 hours after infection as previously described.[14,16] Prepared crude membrane fractions and isolated membrane vesicles were subjected to Western blot analysis. Transport assays were performed using the rapid filtration method previously reported.[14]

Results

Expression of Wild-Type and Two Mutated BSEP in MDCK II Cells. To examine the cellular localization and transport function of the two mutants (E297G and D482G), we constructed recombinant adenoviruses containing wild-type and mutated BSEP cDNA. Expression of BSEP mRNA in the infected MDCK II cells was confirmed via quantitative PCR (Fig. 1). BSEP gene expression was normalized by the expression of β-actin. It was found that the BSEP mRNA expression levels were similar between the wild-type and the two mutants.

The expression level of BSEP was further examined via Western blot analysis (Fig. 2A). It was found that the expression levels of these two mutants were lower than

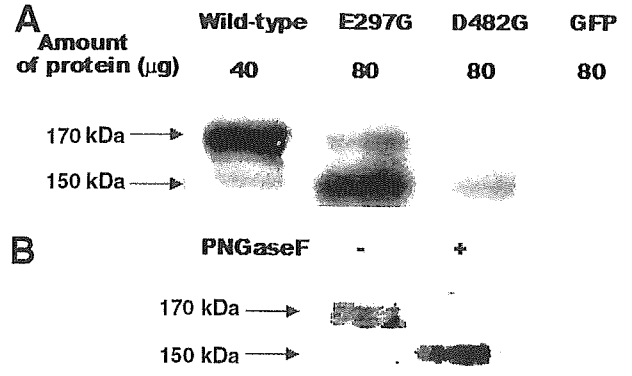

Fig. 2. Determination of expression levels of BSEP. The expression level of BSEP was determined via Western blot analysis. (A) Results of Western blot analysis with crude membrane fraction prepared from MDCK II cells. MDCK II cells were infected with recombinant adrenoviruses at 250 MOI 48 hours before the experiments. Crude membrane fractions prepared from GFP (control), wild-type, E297G, and D482G BSEP-expressing MDCK II cells (80, 40, 80, and 80 μg protein, respectively) were analyzed. (B) Results of Western blot analysis of crude membrane fraction (40 μg protein) expressing wild-type BSEP before and after peptide N-glycosidase F digestion. GFP, green fluorescence protein.

that of the wild-type BSEP. Although the wild-type BSEP was detected as approximately 170 kDa, D482G BSEP was detected as approximately 150 kDa. In addition, E297G BSEP was detected as approximately 170 kDa and approximately 150 kDa bands. Treatment of wild-type BSEP with peptide N-glycosidase F, which is able to cleave the high mannose- and complex-type sugar chains, resulted in the appearance of a band at approximately 150 kDa (Fig. 2B). These results suggest that D482G BSEP and some of the E297G BSEP molecules are present as immature endoplasmic reticulum (ER)-resident forms.

Cellular Localization of Wild-Type and Two Mutated BSEP in MDCK II Cells. We then examined the cellular localization of wild-type and mutated BSEP in MDCK II cells using the immunofluorescence and cell surface biotinylation methods. Although wild-type BSEP is predominantly localized in the apical membrane at 25 MOI (Fig. 3A), there was very little expression of D482G BSEP in most cells at 25 MOI because of the low expression level, as suggested by Western blot analysis (see Fig. 2A). An increase in the MOI to 250 resulted in significant expression of D482G BSEP, suggesting that D482G BSEP are expressed intracellularly (see Fig. 3A). E297G BSEP was located in both the intracellular compartment and apical membrane at 25 MOI (see Fig. 3A). Typical images from the immunofluorescence study are shown in Fig. 3A. To avoid any selection bias, the immunofluorescence study was performed three times, and many fields were selected in each experiment; we obtained the same results in all experiments (see Fig. 3A).

Furthermore, we examined the cell surface expression of wild-type and mutated BSEP via biotinylation assay in MDCK II cells. Cell surface BSEP was detected in wild-type and E297G-expressing MDCK II cells as the mature form, whereas no D482G BSEP molecules were detectable on the cell surface (Fig. 3B). This result is also consistent with the results of the Western blot analysis of the whole cell lysate in which the mature form of D482G BSEP was not detectable (see Fig. 3B).

Proteasome-Mediated Degradation of Two Mutants. It has been reported that proteasomes play an important role in the degradation of incompletely folded and misfolded protein retained in the ER.[17,18] Because the expression levels of E297G and D482G BSEP were lower than that of the wild-type BSEP—and because it is possible that these mutants are localized in the ER—proteasomes may be responsible for their degradation. To examine this hypothesis, cells were treated with 5 μmol/L MG132, a specific proteasome inhibitor, for 8 hours, and its effects on E297G and D482G BSEP were examined via Western blot anasysis. Western blot analysis showed that MG132 treatment caused the accumulation of immature forms (150 kDa), particularly in E297G and D482G BSEP–expressing MDCK II cells (Fig. 4). These results were also consistent with those obtained via immunofluorescence studies. It was found that MG132 treatment resulted in an increase in the number of wild-type, E297G, and D482G BSEP–expressing cells, and the degree of increase was particularly high for the latter two; in the absence of MG132, the number of E297G BSEP-expressing cells after adenovirus infection was only approximately 25% of those expressing wild-type BSEP, and only a minimal number of cells expressed D482G BSEP. In contrast, in the presence of MG132, the number of cells expressing E297G and D482G BSEP was almost the same as that in wild-type BSEP-expressing cells after infection of adenoviruses at the same MOI (data not shown). In the presence of MG132, E297G and D482G BSEP were predominantly expressed in the intracellular compartment, which is the same as that observed under control conditions (see Fig. 3A). This suggests that the expression level of BSEP is increased by MG132, resulting in an increase in the number of cells, the BSEP expression of which was visualized in the immunofluorescence studies.

Transport Function of Wild-Type and Two Mutated BSEP. The transport function of wild-type and mutated BSEP was studied by examining the ATP-dependent uptake of [^{3}H]taurocholate and [^{14}C]glycocholate into membrane vesicles isolated from HEK 293 cells that were infected with recombinant adenoviruses. Although inside-out membrane vesicles—the ATP-hydrolysis re-

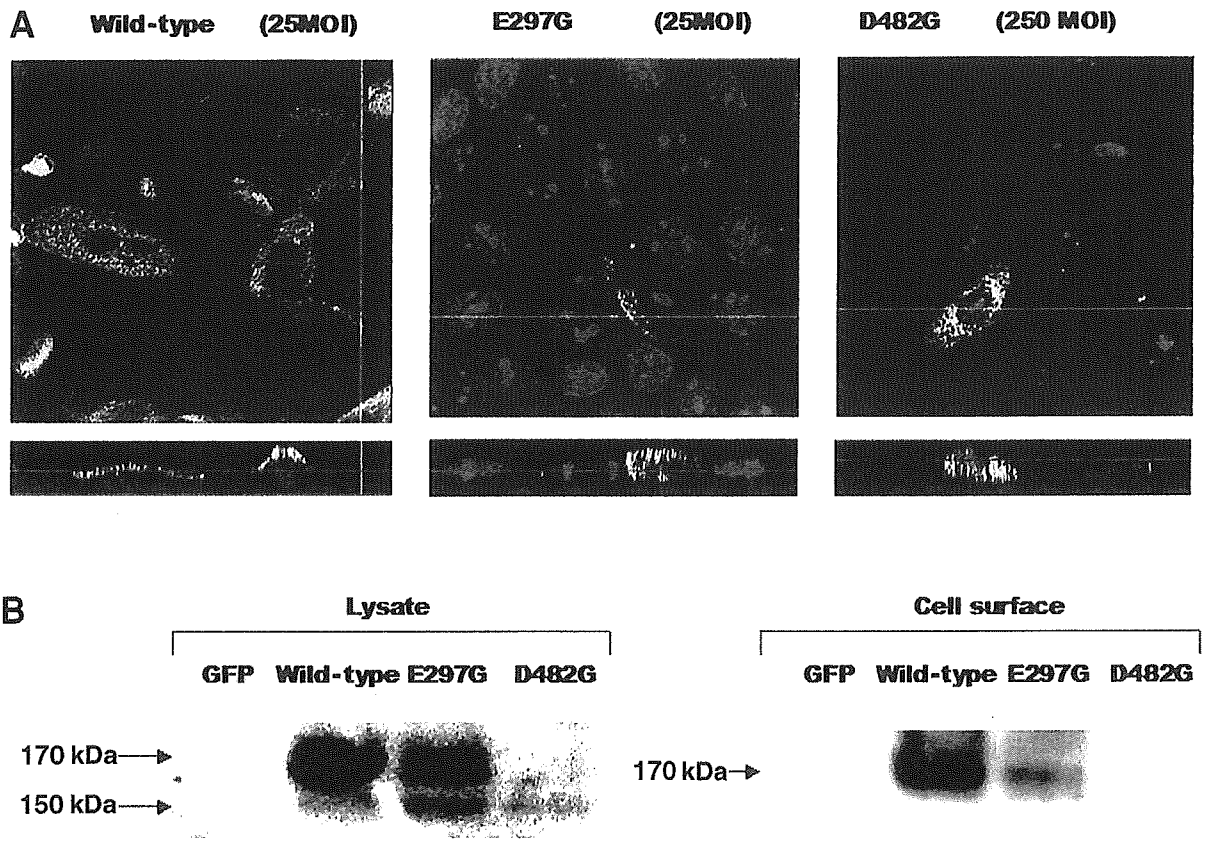

Fig. 3. Localization of BSEP in MDCK II cells. MDCK II cells expressing wild-type and mutated BSEP were analyzed to determine the cellular localization of BSEP by confocal laser scanning microscopy and cell surface biotinylation analysis. (A) Typical results of confocal laser scanning microscopy. MDCK II cells were infected with the recombinant adenoviruses at 25 MOI (wild-type and E297G BSEP) or 250 MOI (D482G BSEP) 48 hours before the experiments. Green and red fluorescence represent BSEP and nuclei, respectively. In each panel, the upper section shows the *en face* image and the lower section shows the vertical image. (B) Results of biotinylation analysis. MDCK II cells were infected with recombinant adenoviruses at 250 MOI 48 hours before the experiments. The cell surface fractions were prepared using the biotinylation method as described in Materials and Methods. The whole cell lysate and biotinylated proteins were subjected to Western blot analysis. MOI, multiplicity of infection; GFP, green fluorescence protein.

gion of which faces to the outside of membrane vesicles—are required to evaluate ATP-dependent transport, it is difficult to prepare inside-out membrane vesicles from MDCK II cells. Consequently, the transport function was studied using isolated membrane vesicles from HEK 293 cells.

Before the transport experiments, the expression level of BSEP was compared among the isolated membrane vesicles expressing wild-type, E297G, and D482G BSEP. D482G BSEP, as well as wild-type and E297G BSEP, were detected as approximately 170-kDa bands in isolated membrane vesicles (Fig. 5A). The band density of the 170-kDa form of E297G and D482G in the isolated membrane vesicles was approximately 25% and 10% of wild-type BSEP, respectively (Fig. 5B). In addition, the degree of expression of the 170-kDa form in the isolated membrane vesicles was twofold higher than that in the crude membrane fractions (Fig. 5C).

The ATP-dependent uptake of taurocholate and glycocholate by wild-type, E297G and D482G BSEP–expressing isolated membrane vesicles was much higher than that by GFP-expressing vesicles (Fig. 6A). By normalizing the BSEP expression levels in the isolated membrane vesicles based on the results of Western blot analysis (see Fig. 5B), it was demonstrated that the transport of taurocholate and glycocholate mediated per unit mass of E297G and D482G BSEP molecules was not significantly different from that by wild-type BSEP (Figs. 5B and 6B). We also performed a kinetic analysis to examine the effect of the two mutations on the transport function of BSEP. Wild-type, E297G, and D482G BSEP–mediated initial ATP-dependent uptake rates were saturable with apparent K_m values of 4.61 ± 0.91, 5.41 ± 0.27, and 14.3 ± 2.0 μmol/L, respectively (Fig. 6C). The maximum taurocholate transport velocity (V_{max}) for wild-type, E297G, and D482G BSEP were 2310 ± 220, 485 ± 15, and 761 ± 60 pmol/min/mg isolated membrane vesicle protein, respectively. By considering the expression level of BSEP in the isolated membrane vesicles (see Fig. 5B), the maximum transport velocity per unit

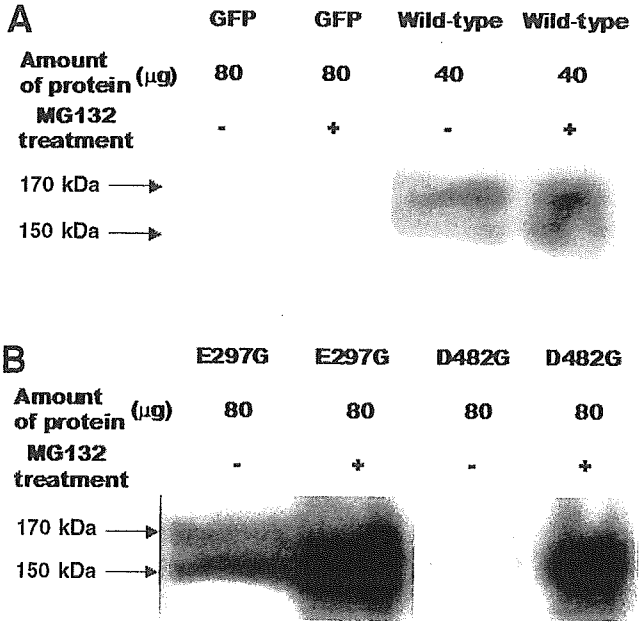

Fig. 4. Effects of proteasome inhibitors on the localization of BSEP in MDCK II cells. MDCK II cells were infected with recombinant adenoviruses at 250 MOI 48 hours before the experiments. Crude membrane fractions prepared from GFP (control), wild-type, E297G, and D482G BSEP-expressing MDCK II cells (80, 40, 80, and 80 μg protein, respectively), treated with or without 5 μmol/L MG132 for 8 hours before the preparation of crude membrane, were subjected to Western blot analysis. GFP, green fluorescence protein.

mass of E297G and D482G BSEP molecules was calculated to be 94% and 329%, respectively, of wild-type BSEP.

Discussion

In the present study, we analyzed the consequence of two frequently found PFIC2 mutations (E297G and D482G) *in vitro* to investigate the pathogenesis of PFIC2. Initially, we examined mRNA and protein levels of wild-type and two mutated BSEP. Although quantitative PCR showed no difference in mRNA levels between the wild-type and two mutated BSEP (see Fig. 1), Western blot analysis indicated reduced expression of D482G and E297G BSEP (see Fig. 2A). In addition, the molecular weight of most of the D482G BSEP and some of the E297G molecules was approximately 150 kDa (see Fig. 2A). Together with the finding that peptide N-glycosidase F treatment of wild-type BSEP results in the appearance of a band at approximately 150 kDa (see Fig. 2B), this suggests that these two mutated BSEP molecules are present as the immature and core-glycosylated form. The absence of glycosylation is consistent with the hypothesis that these mutants are trapped in the ER and are not transferred to the Golgi apparatus where the glycosylation takes place. This suggestion is also consistent with the immunofluorescence observations which indicated that D482G and E297G BSEP molecules are located intracellularly (see Fig. 3A). The results of the surface biotinylation study also suggested that the D482G BSEP and core glycosylated form of E297G BSEP are located intracellularly (see Fig. 3B). In addition, the results of the MG132 treatment experiment suggested that E297G and D482G BSEP molecules are degraded by the proteasome pathway (see Fig. 4). It is possible that the mutated BSEP molecules are degraded by the proteasome pathway after being trapped in the ER, as has been suggested for CFTR ΔF508[17,19] and some MRP2 mutants.[10-12] The impaired BSEP function in PFIC2 patients may also be accounted for by this mechanism. Although the immunohistochemical studies indicate a loss of BSEP on the canalicular membrane in PFIC2 patients with the E297G mutation, we found that some E297G BSEP with a molecular mass of approximately 170 kDa were expressed on the apical membrane (see Fig. 3B). At the present moment, we do not know the reason why some E297G BSEP molecules are trafficked in a normal manner. It is possible that the capacity of the degradation pathway may be saturated due to the high transient expression of BSEP by the adenovirus expression system and, consequently, some of the mutated BSEP molecules are trafficked to the apical membrane. Alternatively, it is also possible that the reduction in the expression level on the apical membrane of E297G BSEP (approximately 25% of wild-type BSEP; see Fig. 3B) may be related to the pathogenesis of PFIC2.

We have also examined the transport function of mutated BSEP using membrane vesicles isolated from HEK 293 cells infected with recombinant adenoviruses. Western blot analysis of the isolated membrane vesicles indicated the presence of approximately 170-kDa molecules for wild-type, E297G, and D482G BSEP. Moreover, it was found that the amount of 150-kDa molecules for E297G and D482G BSEP in the isolated membrane vesicles was lower than that in the crude membrane fraction. It is possible that the isolated membrane vesicles are enriched with the plasma membrane, rather than the membrane fractions from the intracellular compartment. The enrichment of the plasma membrane in the isolated membrane vesicles was confirmed by examining the activity of γ-glutamyltranspeptidase, a plasma membrane marker enzyme. The activity in the isolated membrane vesicles was 1.77 ± 0.60 times higher than that in the crude membrane fraction. This result is consistent with the results of the Western blot analysis, which indicated that the band density of the 170-kDa form of BSEP in the isolated membrane vesicle was approximately twice that in the crude membrane fraction (see Fig. 5C).

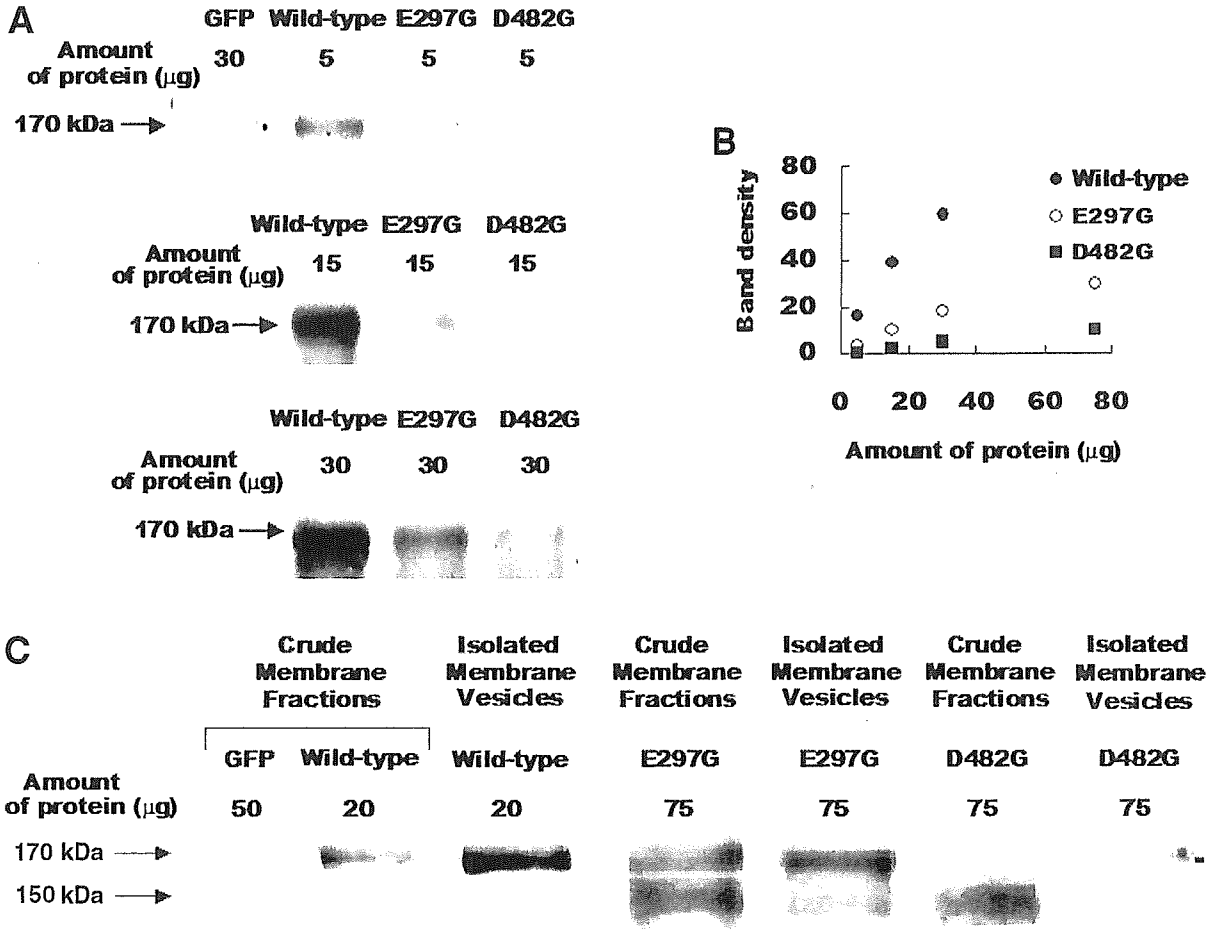

Fig. 5. Expression level of BSEP in isolated membrane vesicles. The expression level of BSEP in isolated membrane vesicles was determined via Western blot analysis. HEK 293 cells were infected with recombinant adrenoviruses at 25 MOI 48 hours before to the experiments. (A) Results of Western blot analysis with isolated membrane vesicles prepared from HEK 293 cells. 5 μg (upper lane), 15 μg (middle lane) and 30 μg (lower lane) protein of isolated membrane vesicles prepared from GFP (control), wild-type, E297G and D482G BSEP-expressing HEK 293 cells were subjected to Western blot analysis. (B) Relationship between the applied amount and the band density. The results for wild-type (●), E297G (○), and D482G (■) BSEP are shown. (C) Results of Western blot analysis using crude membrane fraction and isolated membrane vesicles prepared from GFP (control), wild-type, E297G, and D482G BSEP-expressing HEK 293 cells (50, 20, 75, and 75 μg protein, respectively). GFP, green fluorescence protein.

Functional analysis using these membrane vesicles indicated that the transport of taurocholate and glycocholate in E297G and D482G BSEP–expressing isolated membrane vesicles was significantly higher than that in control isolated membrane vesicles (see Fig. 6A). Based on the hypothesis that the transport activity per unit mass of BSEP molecules can be calculated by considering the BSEP expression level in the isolated membrane vesicles, it was found that the transport of taurocholate and glycocholate mediated per unit mass of E297G and D482G BSEP molecules was not reduced compared with wild-type BSEP (see Figs. 5B and 6B). The K_m values for taurocholate of wild-type, E297G, and D482G BSEP molecules were consistent with previous observations obtained using membrane vesicles isolated from human wild-type BSEP cDNA-infected Sf9 and Sf High Five cells.[2,3] Based on these results, it appears that the transport function of two mutated BSEP molecules (E297G and D482G) *per se* remains normal (see Fig. 6). These results suggest that, if E297G and D482G are matured and consequently expressed on the membrane surface, these mutated transporters are able to transport BSEP substrates.

Our results using mutated human BSEP were different from those reported in a previous study, in which the cause of PFIC2 was examined using mutated rat Bsep,[7] but they were consistent with those reported recently, in which the effect of D482G mutation was examined using mouse Bsep.[8] In the study using rat Bsep gene, the pathogenic mechanism for the D482G mutation was not identified because D482G rat Bsep is localized in the apical membrane as well as the cytoplasm of MDCK cells, and this mutation did not significantly affect taurocholate transport examined using

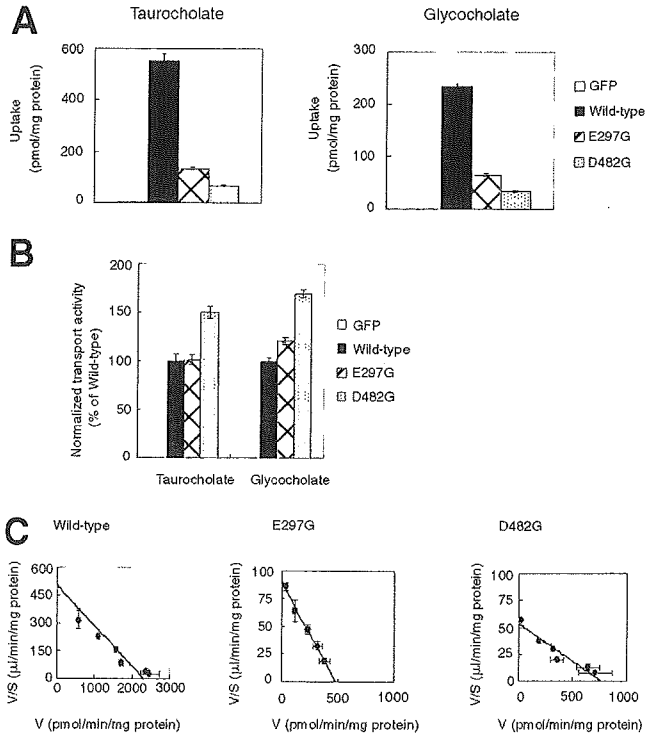

Fig. 6. Transport function of BSEP. Transport function of BSEP was determined using isolated membrane vesicles. HEK 293 cells were infected with recombinant adrenoviruses at 25 MOI 48 hours before the experiments. (A) Uptake of taurocholate (1 μmol/L) and glycocholate (2 μmol/L) into 5 μg protein of isolated membrane vesicles. The isolated membrane vesicles prepared from HEK 293 cells expressing GFP (control) (**white bars**), wild-type (**black bars**), E297G (**cross-hatched bars**), and D482G BSEP (**dotted bars**) were incubated at 37°C for 2 minutes with 5 mmol/L ATP or AMP. The uptake of ligand was obtained by subtracting the value in the absence of ATP from that in its presence. (B) Normalized uptake of taurocholate and glycocholate. The transport activity shown in panel A was normalized by the BSEP expression level shown in Fig. 5B. (C) Saturation of the uptake of taurocholate by the isolated membrane vesicles. The uptake of [^{3}H]taurocholate was examined in the presence and absence of 1.5 to 100 μmol/L of unlabeled taurocholate. Other experimental conditions are described in panel A. Results are given as the Eadie-Hofstee plot for wild-type and mutated BSEP. Each point and vertical/horizontal bar represents the mean ± SE of triplicate determinations. GFP, green fluorescence protein.

membrane vesicles isolated from Sf9 cells.[7] In contrast, in the study with mouse Bsep gene, it was found that D482G mutation resulted in impaired canalicular trafficking in HepG2 cells, although this mutation did not affect the transport of taurocholate examined using membrane vesicles isolated from Sf21 cells.[8] Concerning E297G mutation, it has been shown that E297G rat Bsep is widely distributed throughout the cytoplasm, and the studies using isolated membrane vesicles indicated that this mutation resulted in the loss of taurocholate transport activity.[7] The differences among these results involving the previous mutated rat Bsep, mouse Bsep, and the present mutated human BSEP may be explained by considering the species difference in the Bsep/BSEP sequence, although the homology of the amino acid sequence around E297G and D482G is quite high as far as human BSEP and rat and mouse Bsep are concerned. For example, it is still possible that the introduction of the D482G mutation to human BSEP, but not rat Bsep, results in a conformational change in human BSEP so that D482G BSEP is bound to some molecular chaperons.

The features of D482G BSEP resemble those of the CFTR ΔF508 mutant in that the deletion of phenylalanine at 508 results in the accumulation of the mutated protein in the ER followed by proteasome degradation. In addition, CFTR ΔF508 can transport chloride ions[20] if the mutated transporter is expressed on the plasma membrane. One of the methods being explored as a potential treatment of CFTR ΔF508 patients is to administer drugs (such as sodium 4-phenylbutyrate) which are capable of trafficking the mutated protein to the apical membrane by inhibiting the binding to the molecular chaperons in the ER.[21-23] After clarifying the mechanism for the intracellular retention of E297G and D482G BSEP, it is possible to identify agents able to target these mutated BSEP molecules to the apical surface. Because both of the mutated BSEP molecules *per se* are associated with normal transport functions, it may be possible to treat these PFIC2 patients with such agents.

In conclusion, the results of the present *in vitro* study suggest that E297G and D482G, which are frequently observed PFIC2 mutations, cause deficient BSEP maturation, although the transport functions of these mutants *per se* remain almost normal. These pieces of information should be useful in understanding the pathogenesis of PFIC2.

References

1. Gerloff T, Stieger B, Hagenbuch B, Madon J, Landmann L, Roth J, et al. The sister of P-glycoprotein represents the canalicular bile salt export pump of mammalian liver. J Biol Chem 1998;273:10046-10050.
2. Noe J, Stieger B, Meier PJ. Functional expression of the canalicular bile salt export pump of human liver. Gastroenterology 2002;123:1659-1666.
3. Byrne JA, Strautnieks SS, Mieli-Vergani G, Higgins CF, Linton KJ, Thompson RJ. The human bile salt export pump: characterization of substrate specificity and identification of inhibitors. Gastroenterology 2002; 123:1649-1658.
4. Strautnieks SS, Bull LN, Knisely AS, Kocoshis SA, Dahl N, Arnell H, et al. A gene encoding a liver-specific ABC transporter is mutated in progressive familial intrahepatic cholestasis. Nat Genet 1998;20:233-238.
5. Jansen PL, Strautnieks SS, Jacquemin E, Hadchouel M, Sokal EM, Hooiveld GJ, et al. Hepatocanalicular bile salt export pump deficiency in patients with progressive familial intrahepatic cholestasis. Gastroenterology 1999;117:1370-1379.
6. Thompson R, Strautnieks S. BSEP: function and role in progressive familial intrahepatic cholestasis. Semin Liver Dis 2001;21:545-550.
7. Wang L, Soroka CJ, Boyer JL. The role of bile salt export pump mutations in progressive familial intrahepatic cholestasis type II. J Clin Invest 2002; 110:965-972.
8. Plass JR, Mol O, Heegsma J, Geuken M, de Bruin J, Elling G, et al. A progressive familial intrahepatic cholestasis type 2 mutation causes an un-

stable, temperature-sensitive bile salt export pump. J Hepatol 2004;40:24-30.
9. Cheng SH, Gregory RJ, Marshall J, Paul S, Souza DW, White GA, et al. Defective intracellular transport and processing of CFTR is the molecular basis of most cystic fibrosis. Cell 1990;63:827-834.
10. Keitel V, Nies AT, Brom M, Hummel-Eisenbeiss J, Spring H, Keppler D. A common Dubin-Johnson syndrome mutation impairs protein maturation and transport activity of MRP2 (ABCC2). Am J Physiol Gastrointest Liver Physiol 2003;284:G165-174.
11. Keitel V, Kartenbeck J, Nies AT, Spring H, Brom M, Keppler D. Impaired protein maturation of the conjugate export pump multidrug resistance protein 2 as a consequence of a deletion mutation in Dubin-Johnson syndrome. HEPATOLOGY 2000;32:1317-1328.
12. Hashimoto K, Uchiumi T, Konno T, Ebihara T, Nakamura T, Wada M, et al. Trafficking and functional defects by mutations of the ATP-binding domains in MRP2 in patients with Dubin-Johnson syndrome. HEPATOLOGY 2002;36:1236-1245.
13. Mor-Cohen R, Zivelin A, Rosenberg N, Shani M, Muallem S, Seligsohn U. Identification and functional analysis of two novel mutations in the multidrug resistance protein 2 gene in Israeli patients with Dubin-Johnson syndrome. J Biol Chem 2001;276:36923-36930.
14. Akita H, Suzuki H, Ito K, Kinoshita S, Sato N, Takikawa H, et al. Characterization of bile acid transport mediated by multidrug resistance associated protein 2 and bile salt export pump. Biochim Biophys Acta 2001; 1511:7-16.
15. Suzuki M, Suzuki H, Sugimoto Y, Sugiyama Y. ABCG2 transports sulfated conjugates of steroids and xenobiotics. J Biol Chem 2003;278: 22644-22649.
16. Sasaki M, Suzuki H, Ito K, Abe T, Sugiyama Y. Transcellular transport of organic anions across a double-transfected Madin-Darby canine kidney II cell monolayer expressing both human organic anion-transporting polypeptide (OATP2/SLC21A6) and multidrug resistance-associated protein 2 (MRP2/ABCC2). J Biol Chem 2002;277:6497-6503.
17. Ward CL, Omura S, Kopito RR. Degradation of CFTR by the ubiquitin-proteasome pathway. Cell 1995;83:121-127.
18. Kopito RR. ER quality control: the cytoplasmic connection. Cell 1997;88: 427-430.
19. Gelman MS, Kannegaard ES, Kopito RR. A principal role for the proteasome in endoplasmic reticulum-associated degradation of misfolded intracellular cystic fibrosis transmembrane conductance regulator. J Biol Chem 2002;277:11709-11714.
20. Li C, Ramjeesingh M, Reyes E, Jensen T, Chang X, Rommens JM, et al. The cystic fibrosis mutation (delta F508) does not influence the chloride channel activity of CFTR. Nat Genet 1993;3:311-316.
21. Jiang C, Fang SL, Xiao YF, O'Connor SP, Nadler SG, Lee DW, et al. Partial restoration of cAMP-stimulated CFTR chloride channel activity in DeltaF508 cells by deoxyspergualin. Am J Physiol 1998;275:C171-178.
22. Rubenstein RC, Egan ME, Zeitlin PL. In vitro pharmacologic restoration of CFTR-mediated chloride transport with sodium 4-phenylbutyrate in cystic fibrosis epithelial cells containing delta F508-CFTR. J Clin Invest 1997;100:2457-2465.
23. Rubenstein RC, Zeitlin PL. A pilot clinical trial of oral sodium 4-phenylbutyrate (Buphenyl) in deltaF508-homozygous cystic fibrosis patients: partial restoration of nasal epithelial CFTR function. Am J Respir Crit Care Med 1998;157:484-490.

Available online at www.sciencedirect.com
SCIENCE DIRECT®
Biochimica et Biophysica Acta 1738 (2005) 54 – 62
BIOCHIMICA ET BIOPHYSICA ACTA
BBA
http://www.elsevier.com/locate/bba

Transport by vesicles of glycine- and taurine-conjugated bile salts and taurolithocholate 3-sulfate: A comparison of human BSEP with rat Bsep

Hisamitsu Hayashi [a], Tappei Takada [b], Hiroshi Suzuki [b], Reiko Onuki [a], Alan F. Hofmann [c], Yuichi Sugiyama [a,*]

[a] *Department of Molecular Biopharmaceutics, Graduate School of Pharmaceutical Sciences, The University of Tokyo, 7-3-1 Hongo, Bunkyo-ku, Tokyo 113-0033, Japan*
[b] *Department of Pharmacy, The University of Tokyo Hospital, Faculty of Medicine, The University of Tokyo, Hongo, Japan*
[c] *Department of Medicine, University of California, San Diego, CA 92093-0813, USA*

Received 13 July 2005; received in revised form 17 October 2005; accepted 25 October 2005
Available online 15 November 2005

Abstract

The bile salt export pump (BSEP) of hepatocyte secretes conjugated bile salts across the canalicular membrane in an ATP-dependent manner. The biliary bile salts of human differ from those of rat in containing a greater proportion of glycine conjugates and taurolithocholate 3-sulfate (TLC-S). In the present study, the transport properties of hBSEP and rBsep were investigated using membrane vesicles from HEK293 cells infected with recombinant adenoviruses containing hBSEP or rBsep cDNA. ATP-dependent uptake of radiolabeled glycine-, taurine-conjugated bile salts, and [^{3}H]cholate was observed when hBSEP or rBsep was expressed. Comparison of initial uptake rates indicated that for both transporters, taurine-conjugated bile salts were transported more rapidly than glycine-conjugated bile salts, however, hBSEP transported glycine conjugates to an extent that was approximately 2-fold greater than rBsep. In addition, [^{3}H]TLC-S was significantly transported by hBSEP, and hardly transported by rBsep. The mean K_m value for the uptake of [^{3}H]TLC-S by hBSEP was 9.5±1.5 μM, a value similar to that for hMRP2 (8.2±1.3 μM). In conclusion, both hBSEP and rBsep transport taurine-conjugated bile salts better than glycine-conjugated bile salts, but hBSEP transports glycine conjugates to a greater extent as compared to rBsep. TLC-S, which is present in human bile but not rodent bile, is more avidly transported by hBSEP compared with rBsep.

Keywords: Bile salt; ABC transporter; hBSEP/rBsep

1. Introduction

Bile formation is one of important functions of the liver. Vectorial transport of bile salts from the sinusoidal space to the canaliculus via hepatocytes provides an osmotic driving force for bile formation [1,2]. Transport of bile salts across the sinusoidal membrane is mediated at least in part by both Na^+-taurocholate co-transporting polypeptide (human NTCP/SLC10A1 and rat Ntcp/Slc10a1) [3,4] and Na^+-independent organic anion transporting polypeptides (human OATP/SLCO and rat Oatp/Slco) [1,2]. After reaching the canalicular membrane, monovalent taurine- and glycine-conjugated bile salts are secreted into bile by the bile salt export pump (human BSEP/ABCB11 and rat Bsep/Abcb11) [5–10], whereas sulfated bile salt amidates and bile salt ethereal glucuronides (divalent) are excreted by the multidrug resis-

Abbreviations: BSEP/Bsep, human/rat isoforms of the bile salt export pump; hMRP2/rMrp2, human/rat isoforms of multidrug resistance associated protein 2; hNTCP/rNtcp, human/rat isoforms of Na^+-taurocholate co-transporting polypeptide; hOATP/rOatp, human/rat isoforms of organic anion transporting polypeptide; HEK293, human embryonic kidney 293; PFIC, progressive familial intrahepatic cholestasis; DJS, Dubin-Johnson syndrome; MOI, multiplicity of infection; GFP, green fluorescent protein; TC, taurocholate; GC, glycocholate; CA, cholate; TCDC, taurochenodeoxycholate; GCDC, glycochenodeoxycholate; CDCA, chenodeoxycholate; TUDC, tauroursodeoxycholate; GUDC, glycoursodeoxycholate; UDCA, ursodeoxycholate; TDC, taurodeoxycholate; LCA, lithocholate; TLC-S, taurolithocholate 3-sulfate

* Corresponding author. Tel.: +81 3 5841 4770; fax: +81 3 5841 4766.
E-mail address: sugiyama@mol.f.u-tokyo.ac.jp (Y. Sugiyama).

1388-1981/$ - see front matter © 2005 Elsevier B.V. All rights reserved.
doi:10.1016/j.bbalip.2005.10.006

tance associated protein 2 (human MRP2/ABCC2 and rat Mrp2/Abcc2) [11–13].

The transport properties of hBSEP/rBsep and hMRP2/rMrp2 have been clarified recently. The function of hBSEP/rBsep has been characterized by examining the ATP-dependent transport of taurine- and glycine-conjugated bile salts in isolated bile canalicular membrane vesicles (CMVs) and/or membrane vesicles isolated from hBSEP/rBsep-expressing cells [5–8]. For hMRP2/rMrp2, the transport characteristics have been mainly investigated by comparing transport across the bile canalicular membrane in normal rats with that in Mrp2-deficient rats [8,14–16]. Mutations in BSEP gene are now known to be the cause of progressive familial intrahepatic cholestasis type 2 (PFIC2) [17–21], whereas mutations in MRP2 are the cause of Dubin–Johnson syndrome (DJS) [22–24].

Major bile salts in mammals, i.e., ionized forms of C24-bile acids, are synthesized from cholesterol in the liver and then conjugated (N-acylamidated) with glycine or taurine. In health, sulfation of primary bile salts does not occur in most mammals, but in cholestasis at least in some species, bile salts are extensively sulfated and eliminated into urine. The biliary bile salt composition in the human significantly differs from that in the rat. In humans, the majority of bile salts are conjugated with glycine, whereas in rats, most bile salts are conjugated with taurine. Human bile, but not rat bile, contains sulfated and unsulfated amidates of lithocholate (LCA) [25,26].

Two groups have attempted to relate the transport properties of hBSEP to biliary bile salt composition in humans as compared to that in rats [5,7]. Noe et al. concluded that the transport property of hBSEP/rBsep does not explain the differences in steady state biliary bile salt composition between the two species, because of the similarity of K_m value and intrinsic clearance value for TC, GC, TCDC and TUDC [7]. On the other hand, Byrne et al. concluded that the transport properties of hBSEP/rBsep do in fact correlate with the different bile salt pools in human and rat due to the difference of the relative affinities for TC, GC, TCDC and GCDC between hBSEP and rBsep [5]. In the present study, we have characterized the transport function of hBSEP and rBsep for twelve physiologic bile salts including several kinds of bile salts untested in the previous reports, such as taurolithocholate 3-sulfate. The transport function was determined using membrane vesicles from HEK293 cells infected with recombinant adenoviruses containing hBSEP and rBsep cDNA. We were able to confirm that the transport properties of hBSEP/rBsep reflect the difference in bile salt composition between human and rat. Kinetic analyses to hBSEP and hMRP2 were also performed for [^{3}H]TLC-S, since the initial uptake study demonstrated that this sulfated bile salt is good substrate for hBSEP, not good substrate for rBsep.

2. Materials and methods

2.1. Materials and cell culture

[^{3}H]cholate (CA) (24.5 Ci/mmol), [^{3}H]taurocholate (TC) (2 Ci/mmol), [^{14}C]chenodeoxycholate (CDCA) (48.6 mCi/mmol) and [2-^{3}H]taurine (30.3 Ci/mmol) were purchased from NEN Life Sciences Products (Boston, MA). [^{14}C]glycocholate (GC) (57.3 mCi/mmol) and [^{14}C]lithocholate (LCA) (57.3 mCi/mmol) were purchased from American Radiolabeled Chemicals, Inc. (St. Louis, MO). [^{3}H]ursodeoxycholate (UDCA) (20 Ci/mmol), [^{3}H]tauroursodeoxycholate (TUDC) (10 Ci/mmol), [^{3}H]glycoursodeoxycholate (GUDC) (11 Ci/mmol), [^{3}H]taurochenodeoxycholate (TCDC) (10 Ci/mmol), [^{3}H]glycochenodeoxycholate (GCDC) (11 Ci/mmol) and [^{3}H]taurodeoxycholate (TDC) (29 Ci/mmol) were synthesized in the laboratory of Alan F. Hofmann as described elsewhere [27]. The tritium label was at C-22 and C-23 and has been shown to be stable during hepatocyte transport [28]. [^{3}H]TLC-S was synthesized from lithocholate 3-sulfate using [2-^{3}H]taurine (30.3 Ci/mmol) as described previously [16]. Unlabeled UDCA, TUDC and GUDC were kindly provided by Mitsubishi Pharma (Osaka, Japan). All other chemicals used were commercially available and of reagent grade.

Antiserum for rBsep was raised in rabbits against an oligopeptide (the carboxyl terminal of rBsep; AYYKLVITGAPIS) [29].

Human embryonic kidney (HEK) 293 cells were cultured in Dulbecco's modified Eagle medium (Invitrogen, Carlsbad, CA) supplemented with 10% FBS, penicillin (100 U/ml) and streptomycin (100 U/ml) at 37 °C with 5% CO_2 and 95% humidity.

2.2. Generation of recombinant adenovirus

Full-length hBSEP, rBsep, and hMRP2 cDNAs were cloned as described previously [17,29,30]. The cloned hBSEP, rBsep and hMRP2 cDNAs were introduced into Adeno-X™ viral DNA (Clontech, Palo Alto, CA). The recombinant adenoviruses were produced using the adenovirus expression system according to the manufacturer's instructions, and the titer was examined by an Adeno-X Rapid Titer Kit (Clontech). As a control, recombinant adenoviruses containing green fluorescence protein (GFP) were used.

2.3. Transport studies with membrane vesicles

In order to determine the transport function of hBSEP, rBsep and hMRP2, HEK293 cells were seeded 72 h before infection at a density of 4.0×10^6 cells per 15 cm dish, and infected with recombinant adenovirus at 25 MOI. The isolated membrane vesicles were prepared 48 h after infection as described previously [17]. Transport assays were performed using the rapid filtration method as reported previously [17].

2.4. Western blot analysis

The isolated membrane vesicles were prepared as described above and dissolved in 3 × SDS sample buffer (New England BioLabs, Beverly, MA). The specimens were separated on a 7% SDS-PAGE, and subjected to Western blot analysis with a 1000-fold diluted anti-rBSEP serum as described previously [17].

3. Results

3.1. Uptake of [^{3}H]TC into membrane vesicles

The expression of hBSEP or rBsep in the membrane vesicles prepared from the transfected HEK293 cells was confirmed by Western blot analysis (Fig. 1). As shown in

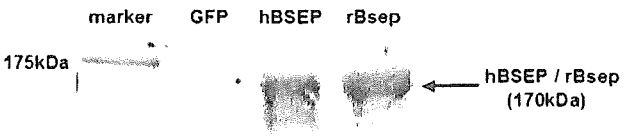

Fig. 1. Western blot analysis of hBSEP and rBsep. Membrane vesicles (15 μg) isolated from hBSEP-, rBsep- and GFP-transfected HEK293 cells were separated on a 7% SDS-PAGE. The proteins transferred to the polyvinylidene difluoride membrane by electroblotting were detected by polyclonal anti-rBsep antiserum.

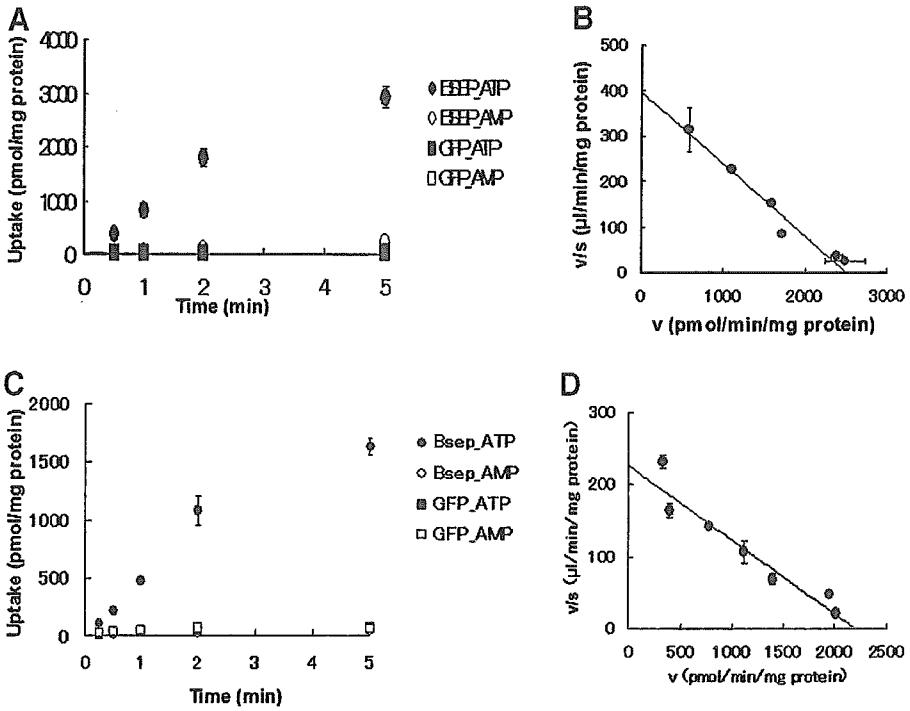

Fig. 2. Uptake of [^{3}H]TC by hBSEP and rBsep. A and C show the time profile for the hBSEP-mediated (A) and rBsep-mediated (C) uptake of [^{3}H]TC. Membrane vesicles (5 μg) prepared from hBSEP-transfected (circles), rBsep-transfected (circles) and GFP-transfected (squares) HEK293 cells were incubated at 37 °C with 5 mM ATP (closed symbols) or AMP (open symbols) in medium containing 0.8 μM [^{3}H]TC and 1.2 μM TC. B and D show the saturation of the hBSEP-mediated (B) and rBsep-mediated (D) uptake of [^{3}H]TC. The uptake of 0.8 μM [^{3}H]TC by hBSEP- and rBsep-expressing membrane vesicles (5 μg) was determined at 37 °C for 2 min with 5 mM ATP or AMP in medium containing 1.5–100 μM of TC. The ATP-dependent uptake was obtained by subtracting the values in the absence of 5 mM ATP from those in the presence of ATP. Results are shown as in an Eadie–Hofstee plot. The solid line represents the fitted line obtained by non-linear regression analysis. Each point and bar represents the mean±S.E. of triplicate determinations.

Fig. 1, hBSEP and rBsep were detected as an approximately 170 kDa form in the fraction of membrane vesicles prepared from hBSEP- and rBsep-transfected HEK 293 cells. No expression of hBSEP or rBsep was detected in the control membrane vesicles prepared from GFP-transfected HEK293 cells.

The time-profiles for the uptake of [^{3}H]TC into the membrane vesicles are shown in Fig. 2A and C. The ATP-dependent uptake of [^{3}H]TC into the membrane vesicles markedly depended on the expression of hBSEP and rBsep. Compared with GFP-transfected HEK 293 cells, the uptake of [^{3}H]TC was linear up to 2 min and was 238-fold and 128-fold higher at 2 min in hBSEP- and rBsep-transfected HEK293 cells, respectively.

A kinetic analysis revealed that the ATP-dependent uptake of [^{3}H]TC into hBSEP-expressing membrane vesicles could be described by a single saturable component with K_m=6.2±0.7 μM and V_{max}=2510±220 pmol/min/mg protein. For rBsep, values were K_m=9.7±1.3 μM and V_{max}=2200±110 pmol/min/mg protein (Fig. 2B and D).

3.2. Uptake of a series of bile salts into membrane vesicles

In addition to TC uptake, the uptake of a variety of natural conjugated and unconjugated bile salts into membrane vesicles was characterized for the purpose of examining the difference between hBSEP and rBsep. The hBSEP- and rBsep-expressing membrane vesicles showed significant ATP-dependent uptake for radiolabeled taurine- and glycine-conjugated bile salts and [^{3}H]CA, whereas radiolabeled unconjugated bile salts, except for [^{3}H]CA, were not transported by hBSEP and rBsep (Fig. 3A and B). Of interest, [^{3}H]TLC-S was ATP-dependently transported by hBSEP, but hardly transported by rBsep (Fig. 3A and B). The initial velocity for hBSEP- and rBsep-mediated uptake of bile salts was in the following order, TCDC>GCDC>TDC≒TUDC>TC>GUDC>TLC-S>GC>CA in hBSEP, TCDC>GCDC≒TDC≒TUDC≒TC>GUDC>GC>CA≒TLC-S in rBsep (Fig. 3A and B). For both hBSEP and rBsep, conjugates of CDCA were transported more rapidly than conjugates of CA. In addition, both species transported taurine-conjugated bile salts to a greater extent than glycine-conjugated bile salts.

A comparison of the initial ATP-dependent uptake of a series of bile salts by hBSEP- and rBsep-expressing membrane vesicles is shown in Fig. 4. The values for ATP-dependent uptake rate by hBSEP and rBsep expression as compared with that of GFP control were calculated from Fig. 3A and B. Then, the ATP-dependent uptake for each bile salt by hBSEP and rBsep was normalized to that for [^{3}H]TC by hBSEP and rBsep, respectively (Fig. 4). This figure demonstrates the greater transport of hBSEP for glycine-conjugated bile salts as compared to rBsep, consistent with preferential glycine amidation of bile salts in humans as compared to preferential taurine amidation in rats.

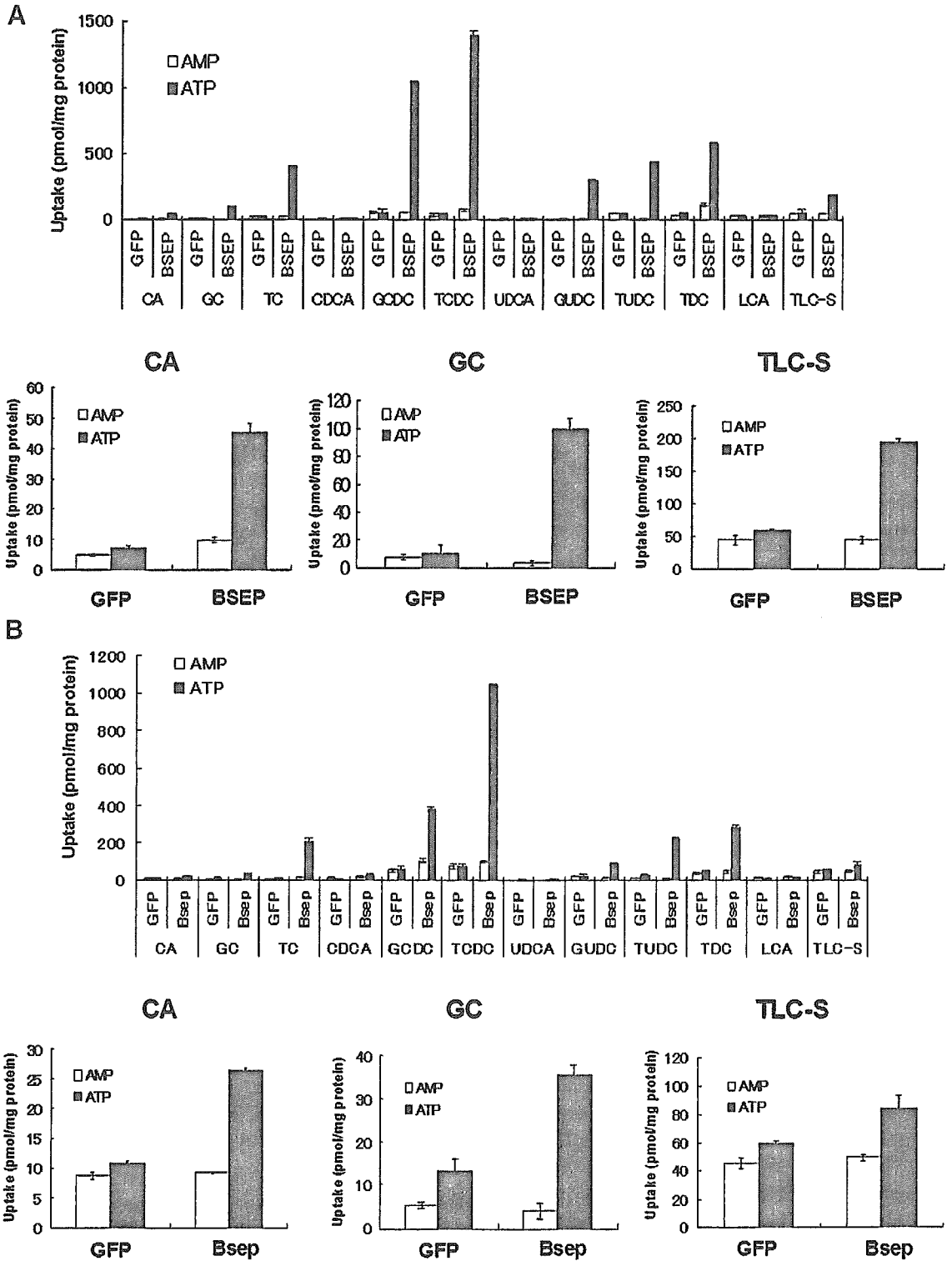

Fig. 3. Initial uptake of a series of bile salts by hBSEP and rBsep. Membrane vesicles (5 μg) prepared from hBSEP-transfected (A), rBsep-transfected (B) and GFP-transfected HEK293 cells were incubated at 37 °C for 30 s with 5 mM ATP (closed columns) or AMP (open columns) in medium containing 2 μM [^{3}H]CA, [^{14}C]GC, [^{3}H]TC, [^{14}C]CDCA, [^{3}H]GCDC, [^{3}H]TCDC, [^{3}H]UDCA, [^{3}H]GUDC, [^{3}H]TUDC, [^{3}H]TDC, [^{14}C]LCA and [^{3}H]TLC-S. Each column and vertical bar represents the mean ± S.E. of triplicate determinations.

Since a species difference was observed for the transport properties of TCDC, GCDC and GC, we performed a kinetic analysis to further characterize the hBSEP- and rBsep-mediated transport of GC, TCDC and GCDC. Like [^{3}H]TC, the ATP-dependent uptake of [^{14}C]GC, [^{3}H]TCDC and [^{3}H]GCDC into hBSEP- and rBsep-expressing membrane vesicles could be described by a single saturable component. The K_m and intrinsic clearance values (V_{max}/K_m) are summarized in the

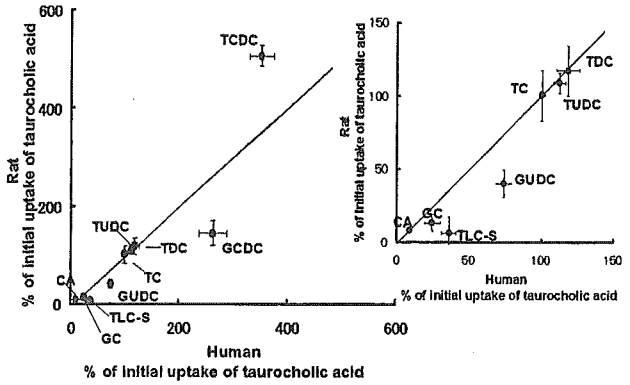

Fig. 4. Comparison of the initial ATP-dependent uptake of a series of bile salts by hBSEP and rBsep. Mean values for the initial ATP-dependent uptake of a series of bile salts (2 μM) by hBSEP and rBsep for 30 s were cited from Fig. 3. The ATP-dependent uptake was obtained by subtracting the values in the absence of 5 mM ATP from those in the presence of ATP. The ATP-dependent uptake for each bile salt by hBSEP and rBsep was normalized with respect to that for TC by hBSEP and rBsep, respectively. Each point and bar represents the mean ± S.E. of triplicate determinations.

Table 1. When the transport rates were expressed as intrinsic clearance values (V_{max}/K_m), the rank order of the extent of the transport rates was TCDC>GCDC>TC>GC in hBSEP and TCDC>GCDC≒TC>GC in rBsep. For the K_m values, no species difference was observed.

3.3. Transport kinetics of [^{3}H]TLC-S

The species difference for TLC-S transport was confirmed by examining the inhibitory effect of TLC-S on the ATP-dependent uptake of [^{3}H]TC by hBSEP- and rBsep-expressing membrane vesicles. The uptake of [^{3}H]TC was inhibited by TLC-S in a concentration-dependent manner with an IC_{50} of 9.0 ± 0.9 μM for hBSEP. For rBsep, the IC_{50} was 52.9 ± 7.9 μM (Fig. 5). The IC_{50} value of TLC-S for [^{3}H]TC uptake by rBsep was comparable with that from our previous study using rBsep-expressing Sf9 membrane vesicles (61.9 ± 19.6 μM) [16].

Transport studies involving [^{3}H]TLC-S using hMRP2-expressing membrane vesicles as well as those using hBSEP-expressing membrane vesicles were performed to compare the affinity of hBSEP for TLC-S with that of hMRP2 which is responsible for the biliary excretion of TLC-S [13,31]. The time-profiles for the uptake of [^{3}H]TLC-S into the membrane vesicles are shown in Fig. 6A and C. There was a marked ATP-dependent uptake of [^{3}H]TLC-S into the membrane vesicles when either hBSEP or hMRP2 was expressed. Compared with GFP-transfected HEK 293 cells, the ATP-dependent uptake of [^{3}H]TLC-S was linear up to 2 min and was 6.2-fold and 5.1-fold higher at 2 min in hBSEP- and hMRP2-transfected HEK293 cells.

A kinetic analysis revealed that the ATP-dependent uptake of [^{3}H]TLC-S into hBSEP- and hMRP2-expressing membrane vesicles could be described by a single saturable component with K_m = 9.5 ± 1.5 μM and V_{max} = 2100 ± 170 pmol/min/mg protein for hBSEP. For hMRP2, values were K_m = 8.2 ± 1.3 μM and V_{max} = 1530 ± 120 pmol/min/mg protein (Fig. 6B and D).

4. Discussion

In the present study, we compared the transport properties of hBSEP and rBsep using membrane vesicles from HEK293 cells infected with adenoviruses containing these cDNAs. Our aim was to examine the correlation between the function of hBSEP/rBsep and the biliary bile salt composition.

Initially, transport studies were performed by measuring the ATP-dependent uptake of [^{3}H]TC into the hBSEP- and rBsep-expressing membrane vesicles to confirm the transport function of hBSEP and rBsep. The K_m values for the hBSEP and rBsep mediated transport of [^{3}H]TC calculated by kinetic analysis were 6.2 μM and 9.7 μM, respectively (Fig. 2). These values are comparable with the previously reported values determined in membrane vesicles from hBSEP- and rBsep-expressing Sf9 cells (4.2 μM [5] and 7.9 μM [7] for hBSEP, 5.3 μM [6] and 7.5 μM [16] for rBsep), and in CMVs (4.2 μM [32] for human and 2.1 μM [33] for rat).

In order to investigate the transport properties of hBSEP and rBsep, we also examined the ATP-dependent uptake of another eleven physiological bile salts, including the bile salts untested in previous reports, by hBSEP and rBsep. Significant ATP-dependent uptake of radiolabeled glycine-, taurine-conjugated bile salts and [^{3}H]CA into hBSEP- and rBsep-expressing membrane vesicles was observed (Fig. 3). rBsep transports [^{3}H]TLC-S less avidly compared with hBSEP (Fig. 3A and B). The rank order determined by the initial velocity (hBSEP: TCDC > GCDC > TDC ≒ TUDC > TC > GUDC > TLC-S > GC > CA, rBsep: TCDC > GCDC ≒ TC ≒ TDC ≒ TUDC > GUDC > GC > CA ≒ TLC-S) (Fig. 3) was identical to that given by intrinsic clearance values (V_{max}/K_m) using K_m and V_{max} values calculated by kinetic analysis (hBSEP: TCDC > GCDC > TC > GC, rBsep: TCDC > GCDC ≒ TC > GC) (Table 1). These results agree closely with the previous studies which showed that the rank orders for the intrinsic clearance values of hBSEP and the initial velocity of rBsep were TCDC > TC > TUDC > GC >> CA ≒ 0 [7] and TCDC > GCDC > TC > TDC ≒ TUDC > GC [8], respectively. The only major difference between the findings of present study and those of the previous study [7] is that CA was not transported by hBSEP in the previous study using membrane vesicles from Sf9 cells. A possible explanation is that the high expression of hBSEP and rBsep by the adenovirus expression

Table 1
Comparison of K_m and V_{max}/K_m values between hBSEP and rBsep

	hBSEP		rBsep	
	K_m (μM)	V_{max}/K_m (μl/min/mg protein)	K_m (μM)	V_{max}/K_m (μl/min/mg protein)
TC	6.2 ± 0.7	400 ± 60	9.7 ± 1.3	230 ± 30
GC	21.7 ± 4.4	78 ± 19	25.7 ± 4.2	47 ± 10
TCDC	6.6 ± 1.2	1300 ± 250	10.2 ± 2.3	820 ± 200
GCDC	7.5 ± 1.0	1000 ± 190	5.6 ± 0.5	240 ± 20

The K_m and V_{max} values for TC were determined by non-linear regression analysis using the data shown in Fig. 2. The K_m and V_{max} values for GC, TCDC, GCDC were determined by the same procedure as that for TC.

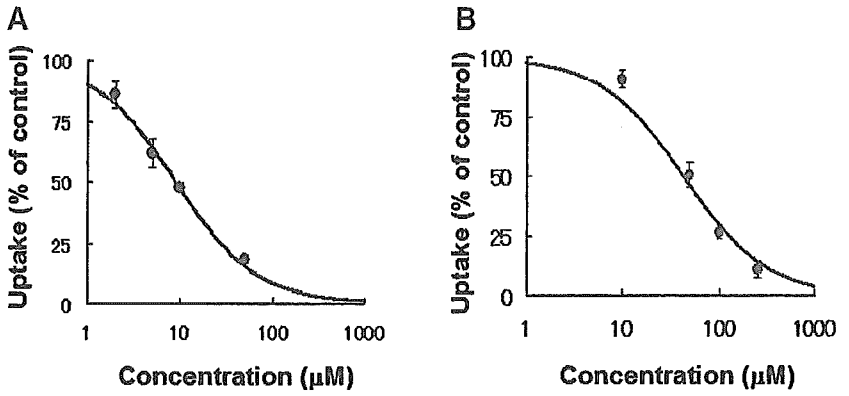

Fig. 5. Inhibitory effect of TLC-S on the ATP-dependent uptake of [^{3}H]TC. [^{3}H]TC uptake by membrane vesicles (5 μg) prepared from hBSEP-transfected (A), rBsep-transfected (B) HEK293 cells was determined at 37 °C for 2 min with 5 mM ATP or AMP in medium containing 0.8 μM [^{3}H]TC, with or without TLC-S at the indicated concentrations. The ATP-dependent uptake values were calculated by subtracting the values in the absence of 5 mM ATP from those in the presence of 5 mM ATP. Each point and bar represents the mean±S.E. of triplicate determinations.

system and/or post-translational modifications of hBSEP and rBsep in our mammalian cell system may have influenced CA transport by hBSEP and rBsep.

The examination using the rank order determined by the initial velocity and intrinsic clearance values hardly showed any species difference in hBSEP/rBsep function. However, a species difference was detected when the ATP-dependent uptake of a series of bile salts was normalized by that of [^{3}H]TC. This quantitative evaluation demonstrated that hBSEP accepted glycine-conjugated bile salts to an extent that was approximately 2-fold greater than rBsep, while there were no differences in the transport properties of taurine-conjugated bile salts, except for TCDC, which was especially well transported by rBsep (Fig. 4). These results indicate that the transport properties of hBSEP/rBsep match the biliary bile salt composition enriched by glycine conjugates in humans compared with rats. In addition, these species difference does not depend on the differences in the affinity for the substrate, since a species difference corresponding to the quantitative evaluation results (Fig. 4) was not observed for the K_m values

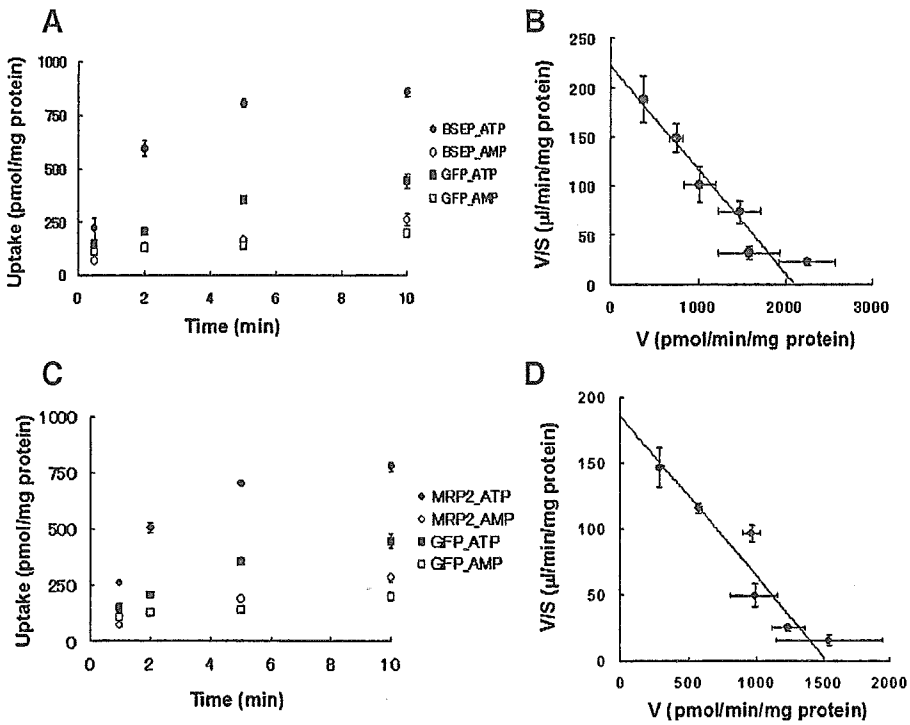

Fig. 6. Uptake of [^{3}H]TLC-S by hBSEP and hMRP2. A and C show the time profile for the hBSEP-mediated (A) and hMRP2-mediated (C) uptake of [^{3}H]TLC-S. Membrane vesicles (5 μg) prepared from hBSEP-transfected (circles), hMRP2-transfected (circles) and GFP-transfected (squares) HEK293 cells were incubated at 37 °C with 5 mM ATP (closed symbols) or AMP (open symbols) in medium containing 1 μM [^{3}H]TLC-S and 1 μM TLC-S. B and D show the saturation of the hBSEP-mediated (B) and hMRP2-mediated (D) uptake of [^{3}H]TC. The uptake of 1 μM [^{3}H]TLC-S by hBSEP- and hMRP2-expressing membrane vesicles (5 μg) were determined at 37 °C for 2 min with 5 mM ATP or AMP in medium containing 0.5–100 μM of TLC-S. The ATP-dependent uptake was obtained by subtracting the values in the absence of 5 mM ATP from those in the presence of ATP. Results are shown as in an Eadie–Hofstee plot. The solid line represents the fitted line obtained by non-linear regression analysis. Each point and bar represents the mean±S.E. of triplicate determinations.

(Table 1). However, these species differences are not enough to explain how the different bile salt composition between human and rat is formed by the species difference of transport properties for hBSEP/rBsep. Most of the bile salts transported by hBSEP and rBsep are recycling bile salts. The steady state composition of the circulating bile salts for amino acid moiety is determined by the balance between the mode of N-acylamidation in the hepatocyte, bacterial deconjugation in the small intestine and the extent of intestinal conservation of the conjugated and unconjugated moieties, as has been reported [34–37].

The result of this study for glycine- and taurine-conjugated bile salts differs only slightly from the previous report by Noe et al. which concluded that the transport properties of hBSEP and rBsep are very similar [7]. Noe et al. characterized the transport properties of hBSEP for TC, GC, TCDC and TUDC, and then examined the species difference in hBSEP/rBsep using K_m values and the rank order of intrinsic clearance values [7], while we characterized the transport properties of hBSEP and rBsep for another eight bile salts in addition to TC, GC, TCDC and TUDC, and then examined the species difference of hBSEP/rBsep by quantitative evaluation (Fig. 4). It is possible that the minor difference between present study and that by Noe et al. is due to the methodological differences, since the results for TC, GC, TCDC and TUDC reported by Noe et al. [7] agreed with those in the present study.

In addition to the glycine- and taurine-conjugated bile salts, TLC-S was ATP-dependently transported by hBSEP, but hardly transported by rBsep (Fig. 3). This species difference was further confirmed by the inhibitory effect on the ATP-dependent uptake of [^{3}H]TC by hBSEP- and rBsep-expressing membrane vesicles (Fig. 5). These results were unexpected. Since, although there have not been any reports examining TLC-S transport by hBSEP, it is generally considered that the biliary excretion of sulfated bile salts is mediated by hMRP2, not hBSEP in humans as well as in rats as described in a number of reports [8,14–16,31]. Several in vivo studies have shown that the biliary excretion of intravenously administered sulfated bile salts amidates were significantly impaired in Groningen Yellow (GY) [14] and Eisai hyperbilirubinemic rats (EHBR) [15] which are Mrp2-deficient rats. Moreover, more direct evidence was provided by in vitro studies showing that the ATP-dependent transport of sulfated bile salts amidates can be observed in isolated bile canalicular membrane vesicles (CMVs) from healthy Sprague–Dawley rats as well as from membrane vesicles isolated from cells transfected with the cDNA for rMrp2. Transport of sulfated bile salts amidates was not observed in CMV from EHBR as well as in membrane vesicles isolated from cells transfected with the cDNA for rBsep [8,16]. Another report described the transcellular transport of TLC-S across MDCKII co-expressing hOATP2 and hMRP2 [31]. Kinetic analysis revealed that the K_m value of TLC-S for hBSEP and hMRP2 was 9.5 μM and 8.2 μM, respectively, indicating that hBSEP and hMRP2 have a similar high affinity for TLC-S (Fig. 6). Thus, there seems convincing evidence that TLC-S is transported by both hMRP2 and hBSEP.

Lithocholate (LCA) is formed in the colon by bacterial 7-dehydroxylation of CDCA and UDCA. It is toxic in animals that lack the ability to detoxify it. In humans, LCA is detoxified by sulfation in hepatocyte which prevents enterohepatic circulation. In rodents, LCA is detoxified by hydroxylation, rather than sulfation [25]. In humans, efficient hepatic elimination of LCA sulfates occurs because of its being a substrate for both hMRP2 and hBSEP. The lack of LCA sulfates in the urine of Dubin–Johnson syndrome patients (our unpublished observations) can now be explained by its being excreted by hBSEP.

hBSEP/rBsep was considered as a specific transporter for monovalent bile salts [5–8,16], although some drugs, such as sulindac, were suggested as potential substrates [38,39]. However, the present study demonstrates that hBSEP accepts the glycine-conjugated bile salts in preference to rBsep and also that hBSEP can transport divalent bile salts such as TLC-S (Fig. 4). This observation has led to the suggestion that hBSEP exhibits a wider substrate specificity than rBsep. Moreover, this suggestion is supported by our recent finding that pravastatin, an HMG-CoA reductase inhibitor, is transported by hBSEP but not rBsep [40]. The importance of the amino acid residues located in the membrane-spanning domains for the substrate recognition of the transporter was previously demonstrated for hMDR1 [41], which belongs to the same subfamily as hBSEP, and rMrp2 [42,43]. Therefore, the cationic amino acids in membrane-spanning domain of hBSEP, such as histidine at 1013 of hBSEP, which are not conserved in that of rBsep may play a key role in the recognition of divalent bile salts.

In conclusion, we demonstrated that hBSEP accepts TLC-S and glycine-conjugated bile salts in preference to rBsep, while there are no differences between hBSEP and rBsep in the transport properties of taurine-conjugated bile salts, except that TCDC is transported more efficiently by rBsep. These results define the substrate specificity of hBSEP compared with rBsep. It seems most probable that hBSEP may be involved in the biliary excretion of endogenous and exogenous substrates other than bile salts.

Acknowledgements

We thank Mr. Masakazu Hirouchi for construction of hMRP2 expression system, Dr. Hidetaka Akita and Ms. Sachiko Mita for construction of rBsep expression system. This work was supported by Grant-in-Aid for Scientific Research on Priority Areas Epithelial Vectorial Transport 12144201 and Grant-in-Aid for Center of Excellence (COE) from The Ministry of Education, Culture, Sports, Science and Technology (MEXT) of Japan. Work in the laboratory of Alan F. Hofmann is supported by NIH Grant DK 64891.

References

[1] P.J. Meier, B. Stieger, Bile salt transporters, Annu. Rev. Physiol. 64 (2002) 635–661.

[2] M. Trauner, J.L. Boyer, Bile salt transporters: molecular characterization, function, and regulation, Physiol. Rev. 83 (2003) 633–671.
[3] B. Hagenbuch, B. Stieger, M. Foguet, H. Lubbert, P.J. Meier, Functional expression cloning and characterization of the hepatocyte Na+/bile acid cotransport system, Proc. Natl. Acad. Sci. U. S. A. 88 (1991) 10629–10633.
[4] B. Hagenbuch, P.J. Meier, Molecular cloning, chromosomal localization, and functional characterization of a human liver Na+/bile acid cotransporter, J. Clin. Invest. 93 (1994) 1326–1331.
[5] J.A. Byrne, S.S. Strautnieks, G. Mieli-Vergani, C.F. Higgins, K.J. Linton, R.J. Thompson, The human bile salt export pump: characterization of substrate specificity and identification of inhibitors, Gastroenterology 123 (2002) 1649–1658.
[6] T. Gerloff, B. Stieger, B. Hagenbuch, J. Madon, L. Landmann, J. Roth, A.F. Hofmann, P.J. Meier, The sister of P-glycoprotein represents the canalicular bile salt export pump of mammalian liver, J. Biol. Chem. 273 (1998) 10046–10050.
[7] J. Noe, B. Stieger, P.J. Meier, Functional expression of the canalicular bile salt export pump of human liver, Gastroenterology 123 (2002) 1659–1666.
[8] B. Stieger, K. Fattinger, J. Madon, G.A. Kullak-Ublick, P.J. Meier, Drug- and estrogen-induced cholestasis through inhibition of the hepatocellular bile salt export pump (Bsep) of rat liver, Gastroenterology 118 (2000) 422–430.
[9] R.M. Green, F. Hoda, K.L. Ward, Molecular cloning and characterization of the murine bile salt export pump, Gene 241 (2000) 117–123.
[10] J. Noe, B. Hagenbuch, P.J. Meier, M.V. St-Pierre, Characterization of the mouse bile salt export pump overexpressed in the baculovirus system, Hepatology 33 (2001) 1223–1231.
[11] H. Suzuki, Y. Sugiyama, Excretion of GSSG and glutathione conjugates mediated by MRP1 and cMOAT/MRP2, Semin. Liver Dis. 18 (1998) 359–376.
[12] J. Konig, A.T. Nies, Y. Cui, I. Leier, D. Keppler, Conjugate export pumps of the multidrug resistance protein (MRP) family: localization, substrate specificity, and MRP2-mediated drug resistance, Biochim. Biophys. Acta 1461 (1999) 377–394.
[13] D. Keppler, J. Konig, Hepatic secretion of conjugated drugs and endogenous substances, Semin. Liver Dis. 20 (2000) 265–272.
[14] F. Kuipers, M. Enserink, R. Havinga, A.B. van der Steen, M.J. Hardonk, J. Fevery, R.J. Vonk, Separate transport systems for biliary secretion of sulfated and unsulfated bile acids in the rat, J. Clin. Invest. 81 (1988) 1593–1599.
[15] H. Takikawa, N. Sano, T. Narita, Y. Uchida, M. Yamanaka, T. Horie, T. Mikami, O. Tagaya, Biliary excretion of bile acid conjugates in a hyperbilirubinemic mutant Sprague–Dawley rat, Hepatology 14 (1991) 352–360.
[16] H. Akita, H. Suzuki, K. Ito, S. Kinoshita, N. Sato, H. Takikawa, Y. Sugiyama, Characterization of bile acid transport mediated by multidrug resistance associated protein 2 and bile salt export pump, Biochim. Biophys. Acta 1511 (2001) 7–16.
[17] H. Hayashi, T. Takada, H. Suzuki, H. Akita, Y. Sugiyama, Two common PFIC2 mutations are associated with the impaired membrane trafficking of BSEP/ABCB11, Hepatology 41 (2005) 916–924.
[18] P.L. Jansen, S.S. Strautnieks, E. Jacquemin, M. Hadchouel, E.M. Sokal, G.J. Hooiveld, J.H. Koning, A. De Jager-Krikken, F. Kuipers, F. Stellaard, C.M. Bijleveld, A. Gouw, H. Van Goor, R.J. Thompson, M. Muller, Hepatocanalicular bile salt export pump deficiency in patients with progressive familial intrahepatic cholestasis, Gastroenterology 117 (1999) 1370–1379.
[19] J.R. Plass, O. Mol, J. Heegsma, M. Geuken, J. de Bruin, G. Elling, M. Muller, K.N. Faber, P.L. Jansen, A progressive familial intrahepatic cholestasis type 2 mutation causes an unstable, temperature-sensitive bile salt export pump, J. Hepatol. 40 (2004) 24–30.
[20] S.S. Strautnieks, L.N. Bull, A.S. Knisely, S.A. Kocoshis, N. Dahl, H. Arnell, E. Sokal, K. Dahan, S. Childs, V. Ling, M.S. Tanner, A.F. Kagalwalla, A. Nemeth, J. Pawlowska, A. Baker, G. Mieli-Vergani, N.B. Freimer, R.M. Gardiner, R.J. Thompson, A gene encoding a liver-specific ABC transporter is mutated in progressive familial intrahepatic cholestasis, Nat. Genet. 20 (1998) 233–238.
[21] L. Wang, C.J. Soroka, J.L. Boyer, The role of bile salt export pump mutations in progressive familial intrahepatic cholestasis type II, J. Clin. Invest. 110 (2002) 965–972.
[22] C.C. Paulusma, M. Kool, P.J. Bosma, G.L. Scheffer, F. ter Borg, R.J. Scheper, G.N. Tytgat, P. Borst, F. Baas, R.P. Oude Elferink, A mutation in the human canalicular multispecific organic anion transporter gene causes the Dubin–Johnson syndrome, Hepatology 25 (1997) 1539–1542.
[23] K. Hashimoto, T. Uchiumi, T. Konno, T. Ebihara, T. Nakamura, M. Wada, S. Sakisaka, F. Maniwa, T. Amachi, K. Ueda, M. Kuwano, Trafficking and functional defects by mutations of the ATP-binding domains in MRP2 in patients with Dubin–Johnson syndrome, Hepatology 36 (2002) 1236–1245.
[24] V. Keitel, J. Kartenbeck, A.T. Nies, H. Spring, M. Brom, D. Keppler, Impaired protein maturation of the conjugate export pump multidrug resistance protein 2 as a consequence of a deletion mutation in Dubin–Johnson syndrome, Hepatology 32 (2000) 1317–1328.
[25] I.M. Arias, N. Fausto, et al., The Liver, Third ed., Raven press, Ltd., New York, 1994.
[26] Y. Siow, A. Schurr, G.C. Vitale, Diabetes-induced bile acid composition changes in rat bile determined by high performance liquid chromatography, Life Sci. 49 (1991) 1301–1308.
[27] S. Sorscher, J. Lillienau, J.L. Meinkoth, J.H. Steinbach, C.D. Schteingart, J. Feramisco, A.F. Hofmann, Conjugated bile acid uptake by *Xenopus laevis* oocytes induced by microinjection with ileal Poly A+ mRNA, Biochem. Biophys. Res. Commun. 186 (1992) 1455–1462.
[28] W.C. Duane, C.D. Schteingart, H.T. Ton-Nu, A.F. Hofmann, Validation of [22,23-3H]cholic acid as a stable tracer through conversion to deoxycholic acid in human subjects, J. Lipid Res. 37 (1996) 431–436.
[29] S. Mita, H. Suzuki, H. Akita, B. Stieger, P.J. Meier, A.F. Hofmann, Y. Sugiyama, Vectorial transport of bile salts across MDCK cells expressing both rat Na+-taurocholate cotransporting polypeptide and rat bile salt export pump, Am. J. Physiol. Gastrointest. Liver. Physiol. 288 (2005) G159–G167.
[30] M. Hirouchi, H. Suzuki, M. Itoda, S. Ozawa, J. Sawada, I. Ieiri, K. Ohtsubo, Y. Sugiyama, Characterization of the cellular localization, expression level, and function of SNP variants of MRP2/ABCC2, Pharm. Res. 21 (2004) 742–748.
[31] M. Sasaki, H. Suzuki, K. Ito, T. Abe, Y. Sugiyama, Transcellular transport of organic anions across a double-transfected Madin–Darby canine kidney II cell monolayer expressing both human organic anion-transporting polypeptide (OATP2/SLC21A6) and Multidrug resistance-associated protein 2 (MRP2/ABCC2), J. Biol. Chem. 277 (2002) 6497–6503.
[32] H. Wolters, F. Kuipers, M.J. Slooff, R.J. Vonk, Adenosine triphosphate-dependent taurocholate transport in human liver plasma membranes, J. Clin. Invest. 90 (1992) 2321–2326.
[33] B. Stieger, B. O'Neill, P.J. Meier, ATP-dependent bile-salt transport in canalicular rat liver plasma-membrane vesicles, Biochem. J. 284 (Pt. 1) (1992) 67–74.
[34] N.E. Hoffman, A.F. Hofmann, Measurement of bile and acid kinetics by isotope dilution in man, Gastroenterology 67 (1974) 887–897.
[35] N.E. Hoffman, A.F. Hofmann, Metabolism of steroid and amino acid moieties of conjugated bile acids in man: V. Equations for the perturbed enterohepatic circulation and their application, Gastroenterology 72 (1977) 141–148.
[36] A.F. Hofmann, Physiology of the Gastrointestinal Tract, 3rd ed., Raven Press, New York, 1994.
[37] A.F. Hofmann, Detoxification of lithocholic acid, a toxic bile acid: relevance to drug hepatotoxicity, Drug Metab. Rev. 36 (2004) 703–722.
[38] V. Lecureur, D. Sun, P. Hargrove, E.G. Schuetz, R.B. Kim, L.B. Lan, J.D. Schuetz, Cloning and expression of murine sister of P-glycoprotein reveals a more discriminating transporter than MDR1/P-glycoprotein, Mol. Pharmacol. 57 (2000) 24–35.
[39] U. Bolder, N.V. Trang, L.R. Hagey, C.D. Schteingart, H.T. Ton-Nu, C. Cerre, R.P. Elferink, A.F. Hofmann, Sulindac is excreted into bile by a canalicular bile salt pump and undergoes a cholehepatic circulation in rats, Gastroenterology 117 (1999) 962–971.

[40] M. Hirano, K. Maeda, H. Hayashi, H. Kusuhara, Y. Sugiyama, Bile salt export pump (BSEP/ABCB11) can transport a non-bile acid substrate, pravastatin, J. Pharmacol. Exp. Ther. 314 (2005) 876–882.
[41] T.W. Loo, D.M. Clarke, Merck Frosst Award Lecture 1998. Molecular dissection of the human multidrug resistance P-glycoprotein, Biochem. Cell. Biol. 77 (1999) 11–23.
[42] K. Ito, H. Suzuki, Y. Sugiyama, Single amino acid substitution of rat MRP2 results in acquired transport activity for taurocholate, Am. J. Physiol.: Gastrointest. Liver Physiol. 281 (2001) G1034–G1043.
[43] K. Ito, H. Suzuki, Y. Sugiyama, Charged amino acids in the transmembrane domains are involved in the determination of the substrate specificity of rat Mrp2, Mol. Pharmacol. 59 (2001) 1077–1085.

7

2）抗がん剤の効果・副作用に関連する薬物代謝酵素・トランスポーターの遺伝子多型

（1）はじめに

旧来より，薬物の効果・副作用には，個人差が存在することが経験的に知られており，現在では，その要因として，薬物動態学的な要因（pharmacokinetics）と，薬動力学的な要因（pharmacodynamics）の２つに大別して考えるのが一般的である．すなわち前者は，投与薬物の循環血中ならびに標的組織中の経時的な濃度推移の個人差であり，それらは，各組織において吸収・分布・代謝・排泄を担う，代謝酵素・トランスポーターなどの機能・発現の個人差と考えることができる．

一方，後者は，同じ薬物濃度で暴露された標的細胞であるにも関わらず効果の強度にみられる個人差であり，薬物の標的レセプターやその下流にあるシグナル伝達分子や転写因子などの機能・発現変化に起因するものと考えられる（**図1**）．特に，抗がん剤がターゲットとする悪性腫瘍については，腫瘍内血管形成の不均一さなどにより，抗がん剤自身の暴露が腫瘍内の細胞によって異なることや，栄養分や酸素の供給など１つの腫瘍内でも個々の細胞を取り巻く環境は異なっており，それに伴い細胞により標的関連分子の発現も異なると考えられている．また，腫瘍細胞は，宿主の遺伝的背景の個人差以外に，薬剤耐性などに関与する薬物排出トランスポーターや標的分子の遺伝子変化をしば

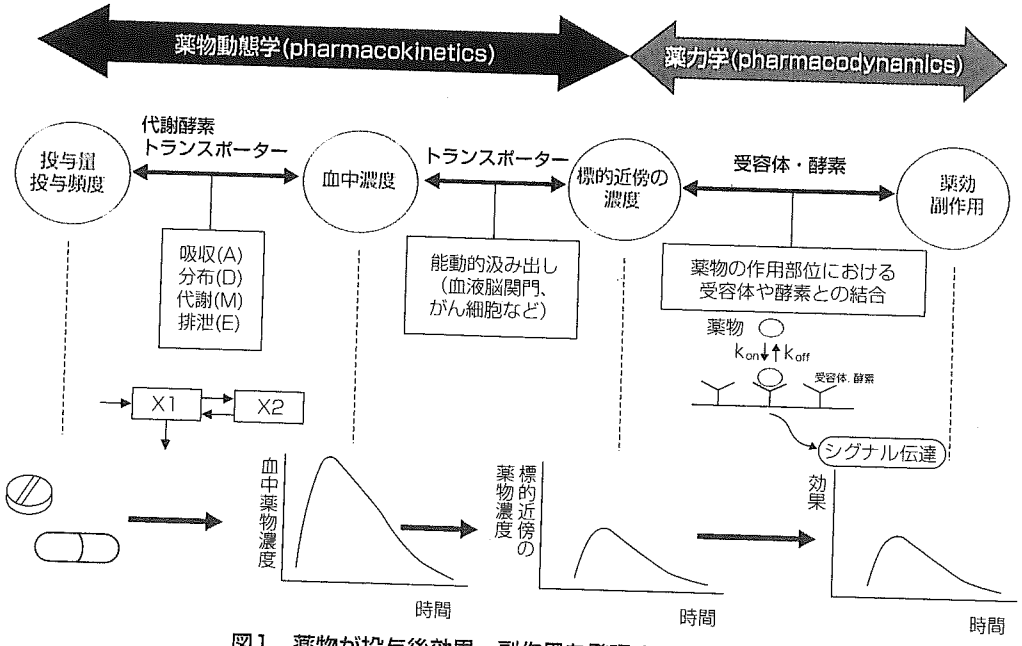

図1　薬物が投与後効果，副作用を発現するまでの過程
（佐藤　均，ファーマコキネティクス　演習による理解，杉山雄一・山下伸二・加藤基浩　編，南山堂より改変引用）

しば後天的に獲得することが知られている．したがって，腫瘍における薬物の暴露や効果を決定する遺伝子の変異は，個人差よりはむしろ腫瘍細胞ごとに異なると考えられる．

一方，薬物の全身における薬物動態を支配する分子の機能・発現は，個人の普遍的な遺伝的背景に支配されており，容易にタイピングをすることが可能なことから，薬物の効果・副作用の個人差を生む要因の一つとして早くから注目を集めてきた．薬物動態に関与する異物解毒系の代謝酵素・トランスポーター群は，いずれも基質認識性が広範であることが多く，一つの分子の機能変化が，複数の薬物の動態に影響を与えることも特徴として挙げられる．特に，抗がん剤においては，濃度―効果曲線を考えた場合，一般の薬物と比較して，治療効果の発現と副作用・毒性発現の濃度域が接近しており，安全域が狭いこと，また副作用が生命の危険を伴うような重篤なものが多いことから，投与する前にあらかじめ薬物動態に関連する分子の機能を遺伝子情報から予測して，個人の代謝・輸送能力に合わせた処方設計を行うことで，全身の薬物動態をコントロールすることは，副作用回避のために最も重要なことであるといえる．また，医薬品開発過程においても，これまでの治験では，投与量が固定されており，結果として，副作用を発現するヒトや効果の無いヒトが混在しており，集団全体としての薬効評価を難しくしていたが，例えば，あらかじめ薬物の効果に関係する遺伝子について診断を行うことで，レスポンダー・ノンレスポンダーを分類することや，代謝酵素・トランスポーターの遺伝子診断により，治療に適切な薬物濃度を確保できるような投与量を層別化して設定することで，適した患者群に対し，適切な処方を通して薬効を最大限引き出すことができると考えられる．本総説では，特に薬物動態を制御する分子群である，代謝酵素・トランスポーターの遺伝子多型と抗がん剤の効果・副作用に与える影響について例を挙げながら，個別化医療への可能性も含め解説する．

(2) thiopurine S-methyltransferase (TPMT)とプリン代謝拮抗薬

プリン代謝拮抗薬である，mercaptopurineやthioguanine，azathiopurineは，それぞれ，リンパ芽球性白血病や骨髄芽球性白血病の症状の寛解に対し汎用されている．これら薬剤は全てプロドラッグであり，細胞内のhypoxanthine phosphoribosyl transferase（HPRT）により一連のthioguanine nucleotidesに変換されて核酸代謝系に拮抗することで活性を示す一方，TPMTによりS-メチル化されることで，不活性化することが知られている．旧来より，患者の一部で，代謝拮抗作用の増強や，重篤な骨髄抑制により投与量の減量をせまられるケースが知られており，現在では，この主原因がTPMTの遺伝子多型による活性の個人差で説明されることが解明されている．Caucasianにおいて，赤血球中のTPMT活性の分布は3峰性を示すことが知られており，全体の約0.3%でTPMT活性がほぼ欠損し，約10%については，残り90%のヒトの半分程度のTPMT活性を示すことが示されている[1]．TPMTの遺伝子解析の進展に伴い，活性が欠損・低下する患者は，TPMT活性がほぼ無くなる遺伝子変異をホモあるいはヘテロで有する患者とほぼ対応することがわかってきた．現在までに，11種類程度のアレルがTPMTの活性低下と関連することが明らかとなってきた（**図2**）．とりわけ，Caucasianにおいては，*TPMT*2*（G238C; Ala→Pro），*TPMT*3A*（G640A+A719G; Ala→Thr+Tyr→Cys），*TPMT*3B*（A719G; Tyr→Cys）の3種類の変異がTPMT活性を減少させるアレルの95%を占めており，これら3種のアレルを調べることでほぼTPMT活性の遺伝子診断が可能であるといえる[2]．これら変異による活性低下の原因は，in vitro実験の結果，いずれも変異TPMTのプロテアソーム系による分解の促進が示唆されている[3][4]．また，TPMT遺伝子の変異には大きな民族差が観察されている．例えば，Caucasianにおいて

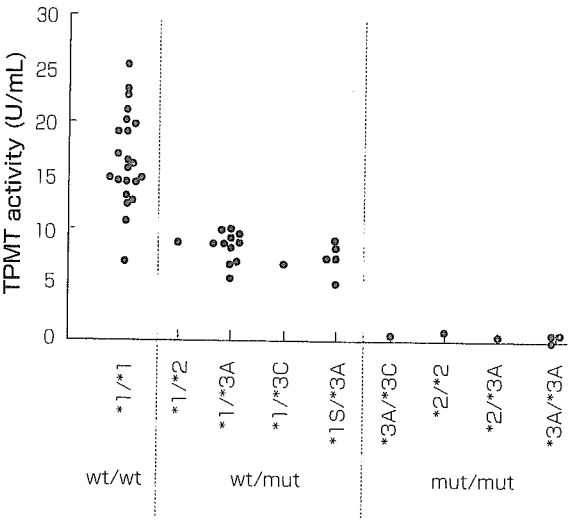

図2　TPMTの遺伝子型と，酵素活性の間の相関
*1が野生型と定義している．
(Yates CR, et al,1997[8] より引用)

は，*3Aが最も多く，4～6%を占めており，ついで，*2, *3Bがそれぞれ0.3～0.8%程度占めている[5,6,7,8]のに対して，Southwest Asian（Indian, Pakistani）においては，*3Aが1%見られるのみで，*2, *3Cは全く見られず[5]，またJapanese, Chineseにおいては，*3Cが0.8%, 2.3%であり，*2, *3Aは見られていない[5) 9)]．さらに最近，野生型アレルをホモで有する患者においてもTPMT活性に数倍のばらつきが観察されており，その原因の候補として，転写開始点から36～116塩基上流にある17～18塩基単位の繰り返し配列の出現回数（4～8回）による転写能力の違いが示唆されている[10]．TPMTの活性については，赤血球における活性と白血病細胞や他の臓器の細胞における活性の間には強い相関が認められていることから，赤血球を用いたTPMT活性の予測は可能だが[11) 12) 13)]，輸血後の患者では，ドナーの血液由来の活性と誤って判断してしまう事例が報告されており[14]，患者の遺伝子診断の方がより正確な判断が可能である．欧米ではTPMT遺伝子診断キットが販売され，実際の医療において，投薬前に診断を行い投与設計を行っている施設もある．TPMTの遺伝子多型がプリン代謝拮抗薬に与える影響に関しては，同一の臨床投与量を与えたときに，赤血球内のthioguanine nucleotidesの濃度が，野生型アレルの保有者と比較して，変異型アレルのヘテロ，ホモ保有者でそれぞれ，2倍，10倍程度に増加し，それに伴って，血液毒性の発生頻度が有意に高まることが知られている[15]．また，レトロスペクティブな解析の結果，mercaptopurine治療において標準投与量が維持された期間が，野生型TPMTをホモで持つ患者においては，治療期間の84%を占めたのに対し，変異型アレルをヘテロ，ホモで有する患者では，65%, 7%と低下したこと，また，TPMT活性と血球減少の副作用により使用を中止した期間との間に負の相関が見られることが報告されている[16]．したがって，例えば，変異型アレルのホモの保有者は，通常の6～10%の投与量を用いるなど，TPMT遺伝子多型に合わせた投与量の至適化が提唱されている[15]．

(3) dihydropyrimidine dehydrogenase(DPD)とフルオロウラシル系抗がん剤

5-fluorouracil（5-FU）は，ピリミジン代謝拮抗薬であり，乳がんや直腸がんに広く用いられている．本薬物もプロドラッグであり，細胞内で5-fluoro-2-deoxyuridine monophosphate（5-FdUMP）がピリミジン合成に必須の酵素であるthymidylate synthase（TS）を阻害することや，一部の3リン酸化体が，DNA, RNAに取り込まれて伸張抑制をすることで殺細胞活性を発揮している．一方，静脈内投与された5-FUのうち約85%は，肝臓中のDPDにより不活化されている．末梢単核球のDPD活性と5-FUの全身クリアランスには正の相関が認められることから，末梢単核球を用いてDPD活性の個人差を議論することが可能であり，その活性の個人差は，約20倍程度と推定されている[17]．また，DPD活性の低い患者においては，活性体である5-FdUMP濃度の上昇とともに，致死的な消化器，血液ならびに神経毒性が発現することが知られている[18,19]．これまで，DPD活性の低い患者において，5-FU投与によるgrade 4の好中球減少のリスクが，通常より3.4倍高くなるとする報告[20]や，副作用発現開始までの期間が2倍短くなるとする報告[21]が見られる．

近年起こったsorivudineと5-FUの相互作用による死亡事故は，sorivudineの腸内細菌による代謝物であるbromovinyl uracilによる非可逆的なDPDの不活化によるものであったこと[22]，また，DPD活性がほぼ欠損している患者において，5-FUの半減期が正常患者と比較して約10倍に遅延したこと[19]を考慮すると，5-FUのクリアランスにおけるDPDの重要性は明らかである．現時点で，DPD遺伝子(*DPYD*)上の変異は，39箇所発見されており，大部分はDPD活性が欠損した患者より発見されたものであることから，機能欠損に関与する変異であるといえる．Caucasianでは，機能欠損した変異DPYDアレルをヘテロ，ホモで有する頻度は，それぞれ3～5%, 0.1%程度である．中でも*DPYD*2A* (IVS14+1G>A)は，機能欠損を示すアレル中50%を占め，exon14のC末側のスプライスドナー部位のmutationによりexon14がスキップされることで活性を持たない変異たんぱく質が産生されるものである[18,23,24]．臨床においても，*DPYD*2*変異をヘテロで有する患者において，5-FUのクリアランスが通常の2.5倍低下していたとする報告[25]や，5-FU投与によりgrade 3～4の重篤な副作用が出た患者60人を対象として，末梢単核球DPD活性ならびに*DPYD*2*変異の有無を調べたところ，DPD活性では，60%の患者において，通常の70%以下に活性が低下しており，うち44%については*DPYD*2*アレルを少なくとも1本有しているという報告がある[26]．一方，DPD活性が保持されている群では，ヘテロの患者1人のみであったことから，*DPYD*2*アレルがDPD活性低下ならびに毒性発現に影響する因子であることが示されている．しかしながら，DPD活性が低下している患者中

でも*DPYD*遺伝子中に変異が見つからないケースがあること[27]，*DPYD*2*の発現頻度に民族差が見られ，Caucasianでは，1～3%程度であるが，JapaneseやAfrican-Americanでは，現在までに見つかっていないことから，DPD活性を遺伝子変異からだけで説明できず[28]，今後の検討が待たれる．また，5-FUの殺細胞活性と，腫瘍のDPD活性が必ずしも相関しないことから，5-FUの治療効果については，標的酵素であるTS遺伝子上流のエンハンサー領域の28塩基の繰り返し配列の回数も関与することが報告されており，薬力学的な遺伝子多型とセットで考えることで効果の個人差を良好に説明できるとされている[29]．

(4) UDP-glucuronosyltransferase (UGT)とirinotecan hydrochloride (CPT-11)

CPT-11は，topoisomerase Ⅰ阻害剤であり，進行性大腸がんに特に効果を示すことから汎用されている．CPT-11はプロドラッグであり，投与後，一部はCYP3A4により不活性代謝物であるAPC, NPCに変換される一方，carboxylesterase-2により活性代謝物であるSN-38を生成する．その後，SN-38は，UGT1A1によりグルクロン酸抱合をうけ，SN-38 glucuronide（SN-38 Glu）となって不活化される．CPT-11は，優れた抗がん活性を示す一方，しばしば患者の一部で，用量規定毒性である致死的な消化管毒性（重篤な下痢など）や白血球減少が見られることが使用を困難にしている．したがって，SN-38の不活化に関わるUGT1A1の遺伝子多型は，SN-38の暴露量，ひいては毒性発現を変化させる要因として重要であろうと考えられる．実際，患者間でSN-38のグルクロン酸抱合活性には，50倍程度の差が観察されている[30]．UGT1A1の活性の個人差を説明しうる最も重要な変異としては，軽度のビリルビン上昇を伴うGilbert's syndromeにおいて見られる*UGT1A1*28*変異があげられる．UGT1A1のexon1前のプロモーター領域にあるTAの反復配列の繰り返し回数は通常6回（(TA)$_6$TAA）であるのに対し，*28変異では，7回（(TA)$_7$TAA）になっており，発現量が低下することが知られている[31]．この配列は，TFIIDという転写因子が結合する場所であることから，*28において転写活性が低下していることが原因と考えられる．実際，UGT1A1の野生型アレルおよび*28変異アレルをそれぞれホモで持つヒトの肝ミクロソームを用いてin vitroでSN-38のグルクロン酸抱合活性を比較したところ，3.85倍の差が見られている[32]．また，臨床では，

表1　白血球減少(Grade 4)もしくは，下痢（Grade 3以上）の副作用発現

	あり (n=26)	なし (n=92)	P
UGT1A1*28			<0.001
+/+	14 (54%)	79 (86%)	
+/−	8 (31%)	10 (11%)	
−/−	4 (15%)	3 (3%)	

UGT1A1*28アレルの保持，非保持を+，−で表した．
(Ando Y, et al, 2000[33] より引用)

CPT-11投与中の患者20人中，3名に重篤な毒性が見られたが，全ての患者が*28変異アレルを少なくとも一つ保持しており[32]，また，好中球の最低数とUGT1A1の遺伝子型との間に相関が見られ，*28アレルが好中球の数を低下させる（すなわち毒性を上昇させる）ことが示唆される事例[32]や，CPT-11投与患者118人中重篤な毒性が26名に見られたが，毒性が見られた患者において，見られなかった患者と比較して，有意に*UGT1A1*28*アレル保持者が多かった事例が報告されている（**表1**）[33]．したがって，*UGT1A1*28*アレルは毒性発現の上昇に寄与していることが示唆される．*UGT1A1*28*のアレル頻度にも民族差が見られており，*UGT1A1*28*だけでは，すべてのSN-38の毒性発現を説明できないのが現状である．UGT1A1の他の変異として，TAの繰り返し回数が5，8回の変異も見つかっており[34]，また，遺伝子内のアミノ酸変異を伴ういくつかの変異も，Gilbert's syndromeを引き起こすことが知られており，これらもSN-38のグルクロン酸抱合活性を変えうる要因になることが今後予想される．

(5) N-acetyltransferase 2(NAT2)とamonafide

Amonafideは，DNAのインターカレート活性とtopoisomerase Ⅱ阻害剤として働き，乳がんや白血病治療薬として開発されていた．本薬物は既に開発が中止されている薬剤であるが，治験のPhase Ⅰの段階で代謝酵素の遺伝子多型を考えた投与量の層別化がなされていた珍しい事例として紹介する[35]．Amonafideは，NAT2により活性を有する代謝物であるN-acetyl-amonafideとなる一方，CYP1A2により活性を持たないN'-oxide-amonafideへと変換される．NAT2の酵素活性には，抗結核薬であるisoniazideの個体差に関連することが知られており，NAT2活性の低いslow acetylatorの存在が知られていた．NAT2活性は，カフェイン摂取後の尿中のアセチル化体と非アセチル化体の比を取ることにより，fast, slow acetylatorを区別している．同一量の